COMPUTATIONAL FLUID DYNAMICS (CFD) IN THAI PATIENTS WITH OBSTRUCTIVE SLEEP APNEA SYNDROME (OSAS) - A CASE REPORT COMPARATIVE STUDY BETWEEN HEALTHY AND OSA SUBJECTS

CHOMPUNUCH SARASAEN

A THESIS SUBMITTED IN PARTIAL FULFILLMENT
OF THE REQUIREMENT FOR THE DEGREE OF
MASTER OF ENGINEERING IN BIOMEDICAL ENGINEERING
FACULTY OF ENGINEERING
KING MONGKUT'S INSTITUTE OF TECHNOLOGY LADKRABANG
2014

KMITL-2014-EN-M-045-161

COMPUTATIONAL FLUID DYNAMICS (CFD) IN THAI PATIENTS WITH OBSTRUCTIVE SLEEP APNEA SYNDROME (OSAS) – A CASE REPORT COMPARATIVE STUDY BETWEEN HEALTHY AND OSA SUBJECTS

CHOMPUNUCH SARASAEN

A THESIS SUBMITTED IN PARTIAL FULFILLMENT
OF THE REQUIREMENT FOR THE DEGREE OF
MASTER OF ENGINEERING IN BIOMEDICAL ENGINEERING
FACULTY OF ENGINEERING
KING MONGKUT'S INSTITUTE OF TECHNOLOGY LADKRABANG
2014

KMITL-2014-EN-M-045-181

หัวข้อวิทยานิพนธ์	พลศาสตร์ของไหลเชิงคำนวณในผู้ป่วยชาวไทย กลุ่มอาการหยุดหายใจขณะหลับเนื่องจากการอุดกั้น – รายงานผลการศึกษาเปรียบเทียบระหว่างคนปกติและคนที่มีภาวะหยุดหายใจขณะหลับ
นักศึกษา	นางสาวชมพูนุช สารแสน
รหัสประจำตัว	54612609
ปริญญา	วิศวกรรมศาสตรมหาบัณฑิต
สาขาวิชา	วิศวกรรมชีวการแพทย์
พ.ศ.	2557
อาจารย์ที่ปรึกษาวิทยานิพนธ์	รศ.ดร. ชูชาติ ปิณฑวิรุจน์

บทคัดย่อ

การศึกษานี้เป็นการเสนอแนวทางการวินิจฉัยแบบใหม่ของภาวะหยุดหายใจขณะนอนหลับเนื่องจากการอุดกั้น โดยใช้พลศาสตร์ของไหลเชิงคำนวณร่วมกับภาพเอ็กซเรย์คอมพิวเตอร์ ภาวะหยุดหายใจขณะหลับเนื่องจากการอุดกั้นเป็นรูปแบบที่พบได้บ่อยของการหยุดหายใจขณะหลับซึ่งได้มีการวิจัยมาเป็นเวลานาน ภาวะนี้ส่งผลกระทบต่อการทำงานของระบบหายใจนำไปสู่ความผิดปกติขั้นรุนแรงที่อาจก่อให้เกิดการเสียชีวิตได้ เช่น โรคหัวใจล้มเหลว หรือโรคหลอดเลือดสมอง เป็นต้น ในปัจจุบันการวินิจฉัยที่เป็นมาตราฐานได้แก่การแปลผลการตรวจการนอนหลับ (polysomnography) แต่อย่างไรก็ตามการวินิจฉัยนี้แสดงเฉพาะข้อมูลเชิงคุณภาพ แพทย์ไม่สามารถตรวจพบบริเวณที่เกิดการอุดกั้นซึ้งเป็นสาเหตุของการหยุดหายใจขณะหลับได้ ดังนั้นเพื่อศึกษาคุณลักษณะของการไหลของอากาศในแบบเรียวไทม์เราจึงประยุกต์ใช้พลศาสตร์ของไหลเชิงคำนวณกับภาพเอ็กซเรย์คอมพิวเตอร์ร่วมกับการแปลผลการนอนหลับในผู้ป่วยชาวไทยรายหนึ่งเพื่อเปรียบเทียบกับคนที่สุขภาพดีอีกสามราย โดยเริ่มจากการนำภาพเอ็กซเรย์คอมพิวเตอร์ที่ทำการคัดแยกส่วนทางเดินอากาศที่ต้องการตั้งแต่รูจมูกถึงคอหอย ผ่านกระบวนการวิศวกรรมย้อนรอยเพื่อสร้างแบบจำลองสามมิติ หลังจากนั้นจึงสร้างเมชให้เป็นส่วนย่อยตามที่ต้องการเพื่อทำการจำลอง ทั้งนี้ได้นำรูปแบบการจำลองการไหลแบบปั่นป่วน k - ε มาใช้ในการวิเคราะห์ เพื่อการศึกษาเชิงเปรียบเทียบลักษณะการไหลของอากาศซึ่งได้แก่ ค่าความเร็วการไหลของอากาศ การกระจายตัวความดัน ค่าความเค้นเฉือน และข้อมูลพื้นที่ตัดขวางของแบบจำลองทั้งหมด ในบริเวณคอหอยหลังช่องปากพบว่ามีค่าความเร็วเพิ่มขึ้นอย่างมากในผู้ป่วยที่มีภาวะหยุดหายใจขณะหลับเนื่องจากการอุดกั้น และค่าความเค้นเฉือนมีค่าสูงขึ้นมากในบริเวณเดียวกัน ปฏิกิริยาระหว่างอากาศที่ไหลผ่านส่วนของผนังโพรงคอหอยที่ซึ่งค่าความดันติดลบนี้เป็นสาเหตุทำให้โพรงอากาศตีบตัว ในงานวิจัยนี้ได้นำเสนอข้อดีของการประยุกต์ข้อมูลพลศาสตร์ของไหลเชิงคำนวณโดยใช้ภาพเอ็กซเรย์คอมพิวเตอร์และการแปลผลการนอนหลับ ซึ่งนอกจากจะสามารถแสดงลักษณะของการไหลของอากาศได้แล้วยังสามารถช่วยในการวินิจฉัยได้เป็นอย่างดี

Thesis	Computational Fluid Dynamics (CFD) in Thai Patients with Obstructive Sleep Apnea Syndrome (OSAS) – A Case Report Comparative Study between Healthy and OSA Subjects
Student	Miss Chompunuch Sarasaen
Student ID.	54612609
Degree	Master of Engineering
Program	Biomedical Engineering
Year	2014
Thesis Advisor	Assoc. Prof. Dr. Chuchat Pintavirooj

Abstract

The new diagnostic approach of obstructive sleep apnea (OSA) using integrated computational fluid dynamics (CFD) based on computed tomography (CT) images are suggested in this study. OSA is one of the most common forms of sleep apnea that has been investigated for several years. It affects a respiratory function which lead to drastic mortality such as heart failure and stroke. Polysomnography (PSG) is now a gold standard test for this symptom. Nevertheless, it provides only qualitative data and physicians cannot determine the obstructed region where the cause of apnea occurs. In order to study airflow behavior for instantaneous monitoring, we used integrated CFD-CT technique with PSG signal in a Thai OSA patient compared with three healthy subjects. First, CT images were segmented from nostril to hypopharynx. Three-dimensional geometrics were then reconstructed by reverse engineering process. Next, mesh generation of models were built to import for numerical simulation which k - ε turbulence model was performed. Flow variables through upper airway, velocity streamline, pressure, wall shear stress (WSS) and cross-sectional area (CSA), were demonstrated for comparison of all models. In oropharynx region, velocity strongly increased in OSA patient that had narrower airway compared with healthy subjects. Large WSS also harshly affects the same site of airway wall. This interaction between flow and the narrowed pharyngeal airway wall may lead to significantly negative pressure that can cause airway to collapse. These factors are essential for analyzing the pathology of airway obstruction. Advantages of combined CFD-CT technique with PSG data has been emphasized in this study. It can be used to illustrated airflow characteristics and utilized as an effective diagnostic tool.

Acknowledgements

This Thesis can be succeeded by the attentive support from my thesis advisor, Assist. Prof. Chuchat Pintavirooj, who gave me invaluable suggestions, continuous encouragement during the period of my study.

I would like to express my sincere gratitude to Assoc. Prof. Jiraporn Laothamatas (M.D.), Assist. Prof. Thongchai Bhongmakapat (M.D.), Assoc. Prof. Manas Sangworasil (Ph.D.), Ms. Khaisang Hemtiwakorn (Ph.D. Candidate), and Ms. Nichapat Chuaychunu for their time and effort in providing CT data and valuable recommendations which make me achieving this success.

I am extremely grateful to Assoc. Prof. Jaruwat Charoensuk and Dr. Bumroong Puangkird for their terrific advices in fluid dynamics and simulation knowledge.

I particularly indebted to Ramathibodi Hospital for their co-operation and supportiveness.

My special thanks also go to Mr. Niwat Phoocharoen, Mr. Thitikarn Okowat, SEAL teams, BIOSIS members and everybody who helped me in this study, gave me an excellent guidance and kind supports until the last moment.

Finally, I would like to thank my family whose patient love enabled me to complete this work. My thesis would not have been finished without their unconditional supports.

Chompunuch Sarasaen

Contents

List of Tables

List of Figures

Figure Page

Chapter I

Introductions

1.1 Statement and significance of the problems

The term of sleep-disordered breathing (SDB) encompasses for wide spectrum of sleep-related breathing disorders (1). Obstructive sleep apnea, also known as OSA, is a potentially serious sleep-disorder breathing in which the person pauses breathing at least 10 seconds or more during sleep (2). It is a life-threatening condition, leading to cardio- and cerebrovascular morbidity (3-5), required immediate attention that everyone can promoted, even if in childhood (6).

The gold standardized test called polysomnography (PSG) (7) is usually performed to diagnose the obstructive sleep apnea (OSA). However, it is a time consuming and expensive procedure. This assessment requires a long wait period in a lab environment through the night with monitoring from a PSG technician. Therefore, it is difficult for patients who lack of their effort and not be aware that they have sleep disorder leading patients more suffer before go to see physicians. Furthermore, a variety of method has been employed for OSA treatment (8-11). Several treatment strategies and surgical procedures are available, but, there is no guarantee of a cure for OSA (12-13).

Moreover, Computational fluid dynamics (CFD) actually has been presented during the few decades. It is a branch of fluid mechanics that uses numerical methods to solve and analyze problems (14). In addition, the finite volume method (FVM); a direct discretization of the control-volume approach. CFD It has gained tremendous fascinating to enable the airflow studies in human upper airways varied from nasal flow structure, OSA in children, drug delivery process to OSA applications, such researches constructing the airway models from medical imaging (15-21). In Thai population, a few of sleep apnea studies (22-25) has been evaluated. The quantitative data that are reported is not enough for cure obstructive sleep apnea proficiently as well.

Owning to these reasons, a new idea of research methodology is accomplished. The propose of this research is Investigating airflow in human upper airways by cooperated computational fluid dynamics with obstructive sleep apnea syndrome based on CT images. Comparing an OSA patient with three healthy subjects in Thai population is proceeded.

The CFD results obtained velocity magnitude, pressure distribution, and wall shear stress which are properties of such airflow. The advantages of this research gain

confidential in diagnostic and treatment planning because of non-invasive technique, accurate qualitative results and cost reductions. That is why the present paper emphasizes on flow behaviors in human upper airway by using computational fluid dynamic coopered with medical imaging of OSA patient. Turbulence model will be adopted for comparison airflow characteristics of OSA and healthy subjects. Therefore, CFD analysis can provide quality assessments for physician in order to evaluate the airflow in patient with OSA.

1.2 Thesis objectives

The specific aims of this study is to suggest a new research methodology in order to OSA diagnosis by combined medical imaging, PSG signal, and CFD analysis for improve diagnosis and the accuracy of treatment planning.

1.3 Hypothesis to be tested

1. CFD and CT images should be well cooperated.

2. Velocity, pressure distribution, wall shear stress and cross-sectional area, could be compared in airflow characteristics between OSA and healthy models effectively.

3. In OSA patient who has narrowed airway, CFD results should indicate more aggressive flow and 3D models could acknowledge the obstructed region exactly.

1.4 Theories or concepts used in the research

In order to solve and analyze the problem such fluid flow, computational fluid dynamics, usually abbreviated as CFD, simulation is employed in this study by using numerical method. The governing equations of fluid flow are the conservation laws of mass, momentum, and energy. In CFD method, Navier-Strokes equations are these set of conservation laws.

Furthermore, the finite volume method known as FVM is a common approach used in CFD codes. FVM is applied to partial differential equations (PDE's) and integral form of the governing equations, conservation law. The domain is discretized into a finite set of control volumes or cells. On each cell, the differential equations are evaluated by a set of algebraic equations.

In finite volume method, values of discrete places are calculated using meshed geometry. So, in FVM, PDE's are converted into surface integrals by using the divergence theorem.

1.5 Scopes of the Study

1. Computational modeling for inspiration was carried out by k - ε turbulence model.

2. Comparing among Thai subjects, i.e., three healthy models and one OSA patient.

3. Introducing new research methodology by combined medical imaging, PSG signal, and CFD analysis for OSAS diagnostic.

4. Using the different flow characteristics including 3D airway models, cross-sectional area, velocity magnitude, pressure distributions, and wall shear stress to developing the accuracy of treatment planning in surgery.

1.6 Thesis Outline

This thesis contents are divided into 6 chapters, that is

Chapters 1 introduced reader to statement of the problem, objectives, hypothesis, scope of the study, process of the study, thesis outline, and the definitions.

Chapters 2 stated obstructive sleep apnea (OSA) essential backgrounds, which comprise of normal upper airway and OSA anatomy, pathogenesis of OSA, diagnosis, and treatments.

Chapters 3 described principles and theories used in this research, which are computational fluid dynamics, governing equations of fluid flow, Navier-Strokes equations, k - ε turbulence model, and also explained finite volume method briefly.

Chapters 4 focused on experimental methods, which are consist of CT data acquisition, airways structure-modeling, reverse engineering process, mesh generation, boundary conditions, numerical simulations, and post-processing.

Chapters 5 indicated results and discussions.

Chapters 6 was conclusions.

1.7 Definitions

AHI	Apnea-hypopnea index
BMI	Body mass index
CFD	Computational fluid dynamics
CPAP	Continuous positive airway pressure
CSA	Cross-sectional area
CT	Computed Tomography
FEM	Finite element method
FVM	Finite volume method
HU	Hounsfield units

LA-PPP	Laser-assisted uvulopalatopharyngoplasty
MMA	Maxillomandibular advancement
MRI	Magnetic resonance image
OSAS	Obstructive sleep apnea syndromes
OSA	Obstructive sleep apnea
PSG	Polysomnography
PDE’	Partial differential equations
SDB	Sleep-disordered breathing
SIMPLE	Semi implicit method for pressure linked equation
STL	Stero lithography
UPPP	Uvulopalatopharyngoplasty
UARS	Upper airway resistance syndrome
WSS	Wall shear stress

Chapter II

Obstructive Sleep Apnea

2. 1 Introduction

Sleep apnea is one of crucial sleep-disordered breathing (SDB). It is characterized by repetitive episodes of either complete airway obstruction (apnea) or partial obstruction (hypopnea) during sleep (2). The word "apnea" means pause in breathing at least ten seconds or up to several minutes, many times through the night (26). Moreover, snoring can be produced when breathing incomplete obstructed, which is usually arise when breathing in more than out. It may be an indicator of violent health conditions such as obstructive sleep apnea although it is often considered as a minor ailment.

The existing types of sleep apnea are central sleep apnea, obstructive sleep apnea (OSA) and mixed or complex sleep apnea (refers to the combination of both central and obstructed sleep apnea). In fact, OSA being the most prevalent at almost 85% (27). Generally, the brain sends a signal to the muscles associated with breathing to take a breath during sleep. Central sleep apnea occur when the brain fails to send the signal properly and then there is no muscular effort to take a breath. Obstructive sleep apnea occur when the brain sends the signal appropriately, however, the muscles are unsuccessful to breath because of the airway obstruction. This study focuses on obstructive sleep apnea since it is the most common form of sleep apnea.

In addition, patients who having obstructive sleep apnea may lead to disrupted sleep, insomnia, and excessive daytime sleepiness. The risk of undiagnosed include heart attack, strokes, congestive heart failure, and hypertension (28-29). Obstructive sleep apnea can be determined by subjective and objective methods. A sleep study called polysomnography (PSG) is the primary objective test for sleep apnea, the gold standardized diagnosis (7). An overnight PSG test measures different biophysiological changes during sleep. The drawbacks of this test regard to a time-consuming and an expensive test.

Normally, OSA can be promoted in children, though it is uncommon, and the prevalence becomes increasing with age. It was acknowledged that approximately 1 in 5 adults that had at least mild OSA and 1 in 15 adults had moderate or severe OSA are affected (30). Additionally, studies reported that men are more likely to suffer OSA than women about four percent and two percent respectively (31-32). During sleep, approximately 22 million Americans suffer from OSA according to American Sleep Apnea Association with about 80 to 90 percent of the moderate-severe sleep apnea

syndrome have been undiagnosed (33). Epidemiology of previous sleep apnea studies informed that African Americans are more likely increase risk compared to Caucasians (34). Besides, Amid African Americans, increase risk factors is unrelated of respiratory conditions or obesity (35). A survey of OSA symptoms among Thai is limited. The first reported case of uvulopalatopharyngoplasty (UPPP), a surgical treatment of OSA, investigated UPPP for excessive snoring, daytime sleepiness, sleep apnea and hypertension in 1988 (22). In 1999, they studied surgical methods for snorers by means of palatal surgery, uvulopalatopharyngoplasty and laser-assisted uvulopalatoplasty (23). In the same year, an early report in Thailand on polysomnography and sleep apnea in adults had been estimated (24). They found the OSA in adult Thai patients, who were suspected of having sleep apnea, more than central and mixed apnea. Polysomnography, In addition, can be a confirmation of symptoms and signs suggestive of OSA and provide a high detection rate. Furthermore, Thai patients had characteristics of OSA similar to patients in the western part of the world. In study by Pongcharusathit C. et al. (25), Clinical predictors of obstructive sleep apnea syndrome had been emphasized in Thai males in 2003 as well. Nevertheless, these previous researches provided only quantitative data. There were no applied with medical imaging or any data related-fields such as fluid dynamics. Neither surgical nor non-surgical treatments cannot ensure that it could completely solve the patients with OSA.

In brief, this study aim to offer a new research methodology for improve OSA diagnosis and surgical treatment by applied computed tomography images, polysomnography, and computational fluid dynamics simulation. The following topics are essential background for better understanding. It begins with normal anatomy of upper respiratory tract and OSA anatomy, pathology, diagnosis, polysomnography, and treatments

2. 2 Normal anatomy of upper respiratory tract and OSA anatomy

Human respiratory system consists of an upper airway and a lower airway depending on, if the respiratory tract is inside or outside of the chest cavity (36). The main passages and structures of the upper airway include nose or nostril, nasal cavity, mouth, paranasal sinuses, throat (pharynx), and voice box (laynx). The lower airway includes the trachea (windpipe), bronchial tubes, and structures inside the lungs as shown in Fig 2.1.

Another definition commonly used in medicine is the airway above the glottis or vocal cords. Some specify that the glottis (vocal cords) is the defining line between the upper and lower respiratory tracts; yet even others make the line at the cricoid cartilage. Upper respiratory tract infections are among the most common infections in the world.

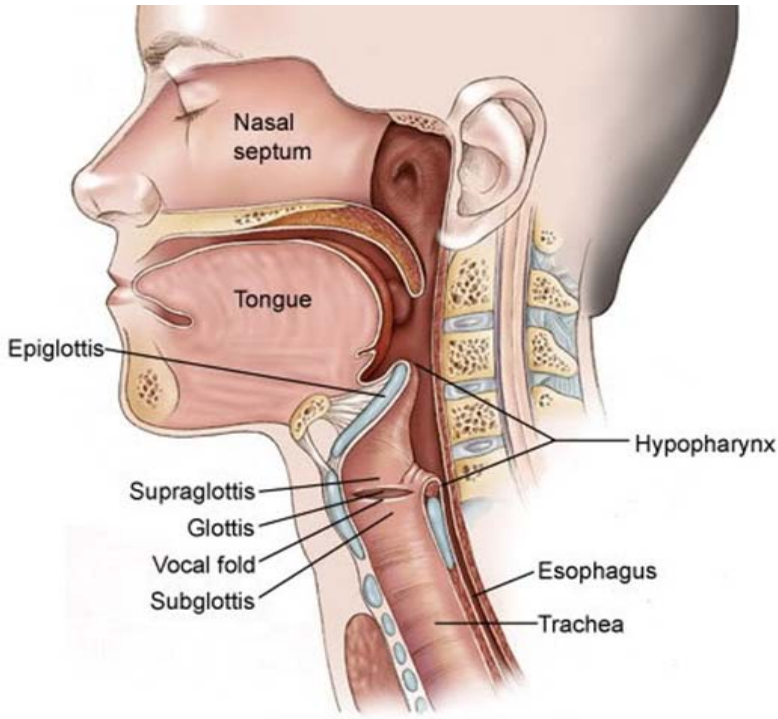

Figure 2.1 Upper respiratory tract (37)

As mentioned above, obstructive sleep apnea is characterized by airway obstruction whether apnea or hypopnea during sleep (2). Comparing the pharyngeal airway between normal anatomical and abnormal (may cause from obstruction) airway is depicted in Fig 2.2. Moreover, two common features, daytime sleepiness and disruption of sleep are caused from increasing ventilatory effort in response to upper airway closure. Risk factors promoted OSA are participated by decrease muscular or neurological tone of upper airway which temporary tonal loss caused from drugs or alcohol and permanent loss could be motivated by traumatic brain injury and neuromuscular disorder. Moreover, increase soft tissue around the airway may obstruct your breathing. It sometimes related with excess weight or narrowed anatomical abnormality (38).

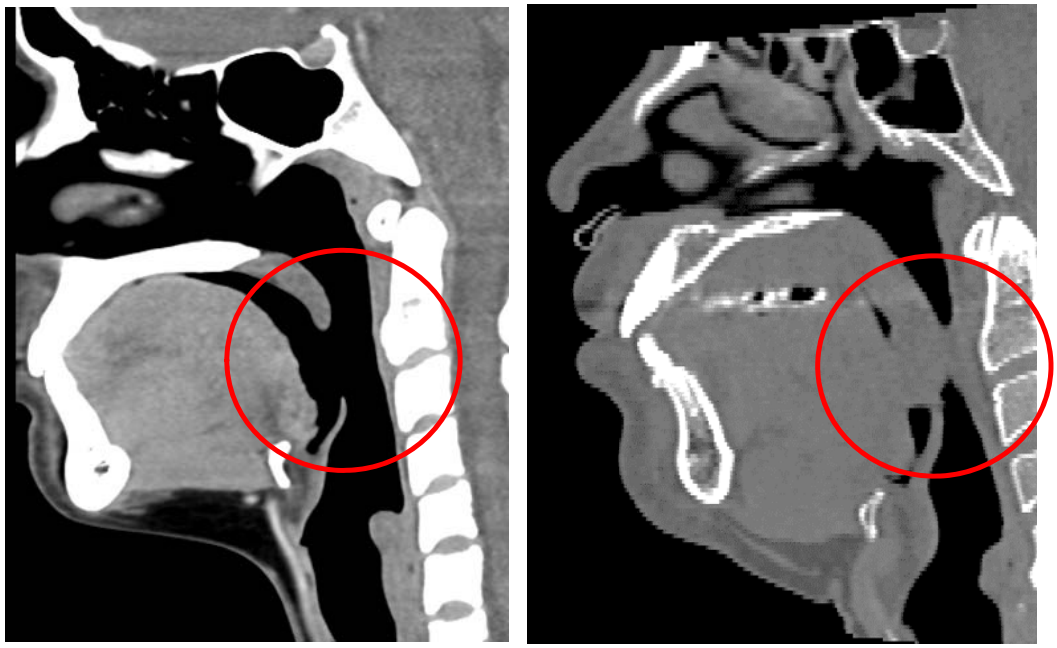

(a) (b)

Figure 2.2 CT image of upper respiratory tract, compare the red circle which is constricted region (a) normal airway structure and (b) abnormal airway structure

Episodes of obstructive apnea and obstructive hypopnea frequently occur in the same patient. Although obstructive apnea may be associated with greater oxyhemoglobin desaturation, distinguishing apnea from hypopnea has little effect on the approach to treatment. Many lab-oratories report the combined number of episodes of apnea and hypopnea per hour of sleep as a single apnea–hypopnea index or respiratory- disturbance index. The upper airway resistance syndrome is character-zed by arousal in response to increased upper airway resistance without an elevated apnea or hypopnea index. Patients with the upper airway resistance syndrome are usually heavy snorers.

2. 3 Pathogenesis

2.3.1 Signs and Symptoms

2.3.1.1 Excessive daytime sleepiness

2.3.1.2 Snoring, nighttime gasping, choking or coughing

2.3.1.3 Insomnia

2.3.1.4 Morning headaches

2.3.1.5 Frequent nocturnal urination

2.3.1.6 Depression

2.3.1.7 Hypertension

2.3.1.8 Obesity

2.3.1.9 Gastroesophageal reflux

2.3.1.10 Large neck size

2.3.1.11 Upper airway or facial abnormalities

2.3.2 Pathogenesis

Upper airway dysfunction and the specific sites of narrowing or closure, such as velopharynx, oropharynx, or hypopharynx, are influenced by the underlying neuromuscular tone, upper-airway muscle synchrony, and the stage of sleep. These events are generally most prominent during rapid-eye-movement (REM) sleep because of the hypotonia of the upper airway muscles characteristic of this stage of sleep.

Patients of normal body weight in whom sleep apnea develops may have tonsillar hypertrophy or craniofacial skeletal abnormalities that also predispose the airway to narrowing or closure during sleep. These craniofacial abnormalities may be evident on a cephalometric radiograph, although not readily apparent on physical examination.

Genetic and environmental factors may also adversely affect airway size. Sleep apnea has been identified as common to some families. The increased incidence of sleep apnea in these families is not explained by obesity alone. Genetically determined craniofacial features or abnormalities of ventilatory control may account for this pattern of familial apnea. If the soft palate is exposed to recurrent vibratory trauma (snoring) and high negative inspiratory pressure, the result can be lengthening of the soft palate due to stretching and thickening caused by edema. It is possible that the changes in the soft palate of patients with sleep apnea may thus be a consequence of breathing against increased upper airway resistance rather than the cause of that increased resistance.

Patients with sleep apnea also have an increased risk of pulmonary hypertension, right and left ventricular failure, myocardial infarction, and stroke. Retrospective studies indicate that there is an association of sleep apnea with morbidity and mortality due to cardiovascular and cerebrovascular causes. The risk of vascular disease appears to be mediated by the complex interaction between the mechanical and chemical effects of repetitive upper airway closure and their effect on the autonomic nervous system. The repetitive increase in sympathetic tone in patients with sleep apnea may be responsible for the development of diurnal hypertension.

Sleepiness, fatigue, irritability, and personality change have been attributed to nocturnal desaturation and the chronic sleep deprivation caused by sleep fragmentation. Sleep fragmentation may be the most important predictor of daytime sleepiness. Patients with sleep apnea are also at increased risk for motor vehicle accidents. The accident rate for such patients has been reported to be seven times that of the general driving population.

2. 4 Diagnosis

Snoring loudly, fatigue, or both are frequently the patient's only symptoms. A focused history taking and physical examination of patients who report such symptoms may aid in identifying persons at risk for sleep apnea. Most patients with sleep apnea are objectively sleepy, although daytime sleepiness is underreported because it generally manifests itself over a prolonged period and patients change their lifestyles gradually to compensate for it.

Other patient characteristics associated with sleep apnea include male sex; age of more than 40 years; habitual snoring; nocturnal gasping, choking, or resuscitative snorting; observed apnea; and a history of systemic hypertension. Symptoms of daytime somnolence, unrefreshing sleep, morning headaches, cognitive impairment, depression, nocturnal esophageal reflux, and nocturia are commonly reported, but do not distinguish sleep apnea from other, nonpulmonary, sleep disorders.

The presence of certain physical characteristics should heighten the physician's suspicion of upper-air-way dysfunction during sleep. Retrognathia and discrete upper airway abnormalities, such as an enlarged soft palate or tonsillar hypertrophy, are clinical clues. An increased body-mass index (the weight in kilo-grams divided by the square of the height in meters), hypertension, and an increased neck circumference (measured at the cricothyroid membrane) are often characteristic of patients with sleep apnea. Increased upper-body obesity, which is reflected by the neck circumference, is a particularly good predictor of sleep apnea.

A sleep study should be strongly considered for two groups of patients: those who habitually snore and report daytime sleepiness, and those who habitually snore and have observed apnea (regardless of daytime symptoms). Polysomnography, in fact, is the gold stand of obstructive sleep apnea diagnosis.

2.4.1 Polysomnography

A type of sleep study is a multi-parametric test used in the study of sleep and as a diagnostic tool in sleep medicine. The test result is called a polysomnogram, also abbreviated PSG as illustrated in Fig 2.3. A sleep study is performed to confirm the presence of upper airway closure during sleep and to

assess the patient's level of risk. A full night of polysomnography, conducted by a technologist in a sleep laboratory, has traditionally been regarded as the gold standard for diagnosing sleep apnea. The polysomnogram is a comprehensive study used to record many physiologic variables in order to diagnose a wide spectrum of pulmonary and nonpulmonary disorders of sleep.

Portable, unattended monitoring systems that can be used outside the hospital promise a more cost-effective alternative to the standard diagnostic nocturnal polysomnography. Whether abbreviated testing, inside or outside the hospital, can successfully establish a diagnosis of sleep apnea is a subject of controversy. Portable systems vary in the manner in which physiologic signals are recorded and scored, as well as in whether cardio-pulmonary variables alone, or sleep and cardiopulmonary variables together, may be monitored. One major concern about the use of portable monitors is that air-flow, ventilatory effort, and arousal may not be measured at all (or may be measured less precisely than in the laboratory) and that the monitors may therefore miss episodes of hypopnea or arousal due to upper-air-way resistance.

Polysomnography is a comprehensive recording of the biophysiological changes that occur during sleep. It is usually performed at night, when most people sleep, though some labs can accommodate shift workers and people with circadian rhythm sleep disorders and do the test at other times of day. The PSG monitors many body functions including brain (EEG), eye movements (EOG), muscle activity or skeletal muscle activation (EMG) and heart rhythm (ECG) during sleep. After the identification of the sleep disorder sleep apnea in the 1970s, the breathing functions respiratory airflow and respiratory effort indicators were added along with peripheral pulse oximetry.

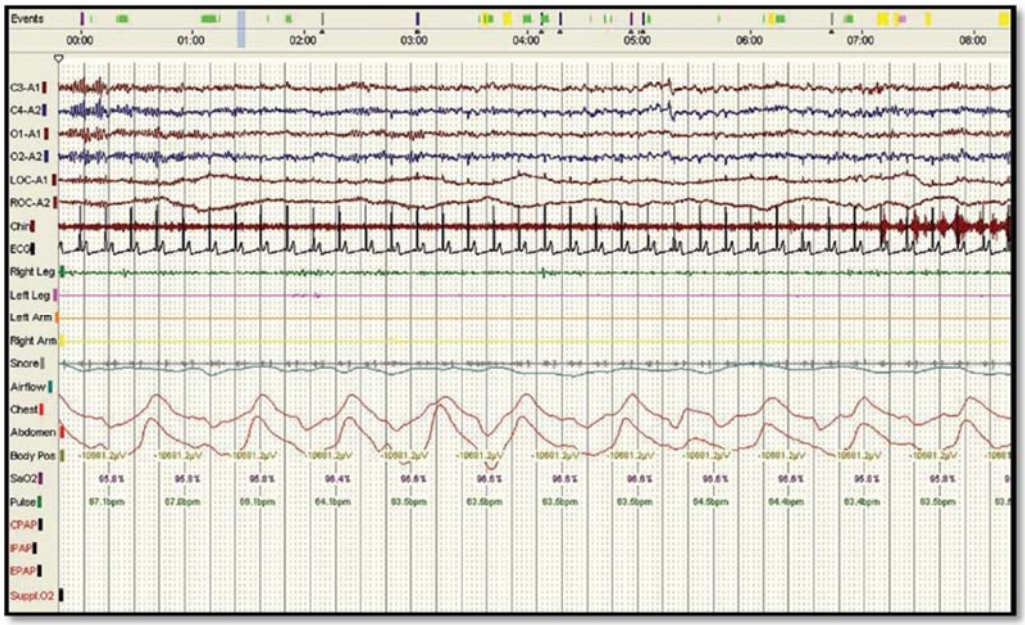

(a)

EEG Rhythm	Characteristics	Best seen	Examples 1s
Posterior Dominant Rhythm (PDR)	8.5-12Hz	Occipital	
Slow Waves	0.5-2Hz; amplitude ≥75μV.	Frontal	
Spindle	11-16 Hz; duration ≥ 0.5s.	Central	
K-Complex	Diphasic; large amplitude, duration ≥ 0.5s.	Frontal	

(b)

Figure 2.3 (a) Polysomnographic recorded data (b) EEG Rhythm

2.4.2 Apnea – Hypopnea Index (AHI)

We can determine the obstructive sleep apnea severity by measured the apnea index (AI) or the apnea-hypopnea index (AHI). AI is defined as the number of apnea repetitions in an hour during sleep. In general, AI of adults is not less than 5 times per hour according to sleep disruption. AHI, similar to AI, combines the number of apneas and hypopneas per hour. The apneas, pauses in breathing, must be recorded at least 10 seconds and are also related with blood oxygen desaturation. Moreover, respiratory disturbance index (RDI) is another index that include AHI and respiratory effort-related arousal (RERA).

The AHI, as with the separate apnea index and hypopnea index, is calculated by dividing the number of events by the number of hours of sleep. In general, AHI values are categorized as 5–14/hr = mild; 15–30/hr = moderate; and > 30/h = severe (1).

2. 5 Treatments

Therapeutic strategies for patients with sleep apnea may be grouped into three general categories: behavioral, medical, and surgical. Treatment decisions should be based on the effect of the sleep disorder on daytime symptoms and cardiopulmonary function rather than on the absolute number of episodes of apnea or hypopnea. The goals of treatment are to establish normal nocturnal oxygenation and ventilation, abolish snoring, and eliminate disruption of sleep due to upper airway closure.

Continuous positive airway pressure (CPAP) is the first choice for OSA treatment because of its non- invasive characteristic. However, the compliance of CPAP is a problem in some of the patients. So, surgery can be considered as the first-line treatment in OSA patients, for whom other non-invasive treatments failed. Surgical treatment of OSA aims to improve the size or tone of a patient's upper airway.

For decades, tracheostomy, including uvulopalatopharyngoplasty (UPPP), laser-assisted uvulopalatoplasty (LAUP) and Maxillomandibular advancement (MMA) etc., was the only effective treatment for sleep apnea and it is particularly effective for Asian people. However, the success rate of upper airway surgery is not good (12-13). The post-operative complications after surgery are often the result of a dilemma during the operation of how much tissue to resect: too little is ineffective, yet too much may leave a patient with speech impedance and palatal stenosis, which can make OSA worse. Therefore, accurate prediction of tissue reduction for this treatment is urgently needed.

2.5.1 Behavioral treatments

All patients with sleep apnea should be counseled about the potential benefits of therapy and the risks of going without treatment. The value of

avoiding factors that increase the severity of upper airway obstruction — such as sleep deprivation; the use of alcohol, sedatives, and hypnotic agents; and increased weight — should be discussed. Alcohol selectively reduces up-per-airway muscle tone and increases the frequency of abnormal breathing during sleep. Alcohol also pro-longs apnea by delaying arousal. In obese patients, weight loss can significantly decrease the severity of the apnea. In some patients, upper airway dysfunction is present only during sleep in the supine position; training these patients to sleep exclusively in the lateral recumbent position may be useful, although the long-term effectiveness of this intervention is unclear. The diagnostic polysomnogram must be carefully analyzed if positional therapy is to be recommended as the sole treatment. A patient's moving from the supine to the lateral recumbent position may make apnea less apparent or convert it to another form of sleep-disordered breathing, hypopnea, or upper airway resistance.

2.5.2 Medical Treatments

2.5.2.1 Airway Pressure

Positive airway pressure, delivered through a mask, is the initial treatment of choice in clinically important sleep apnea. Machines for creating continuous positive airway pressure run on household current, weigh approximately 2 kg (5 lb), and fit easily on a bedside table. The systems cost about $1,000 each. Continuous positive pressure is applied to the upper airway with a nasal mask, nasal prongs, or a mask that covers both the nose and mouth. A pneumatic splint is also provided that prevents narrowing and closure of the upper airway regardless of the site of obstruction. The level of positive pressure required to sustain patency of the upper airway during sleep should be determined in the sleep laboratory.

To decrease the cost of polysomnography and facilitate treatment, some physicians have at-tempted both to diagnose the condition and to initiate treatment with positive airway pressure in a single night of observation. With this approach, an adequate determination of the degree of pressure needed for treatment can be achieved approximately 60 percent of the time. It is unclear, however, how this approach affects the patient's likelihood of accepting and complying with treatment. Subjective estimates of patient compliance are higher than objectively determined values. Patients treated with continuous positive airway pressure delivered nasally have repeatedly demonstrated

improvement in neuropsychiatric function and a lessening of daytime sleepiness. Nocturnal desaturation, ventilatory-related arousals, nocturnal dysrhythmias, pulmonary hypertension, and right-sided heart failure have also been effectively treated. Preliminary data suggest that the treatment can also improve control of diurnal hypertension, probably by correcting nocturnal desaturation and lowering nocturnal catecholamine release. These results parallel those observed after tracheostomy, but continuous positive airway pressure does not entail the morbidity and disfigurement associated with that procedure. Retrospective studies suggest that patients treated with nasally delivered continuous positive airway pressure or tracheostomy have improved survival.

Serious complications of therapy with continuous positive airway pressure are rare. Side effects reported by patients usually involve discomfort or irritation related to the nasal mask. Patients may complain of nasal congestion, dryness, or occasional rhinorrhea. Nasal congestion can be treated with antihistamines or topical corticosteroids. Topical saline sprays or humidification will improve nasal dryness. Some patients may complain of increased resistance to exhalation or a sensation of too much pressure in the nose.

Certain patients become claustrophobic when using positive airway pressure. Changing from a nasal mask to the less confining nasal prongs may alleviate this problem. If this change is not effective, progressive de-sensitization to the mask may be helpful. Optimal treatment with positive airway pressure can also be hampered by air leaks from the mouth that cause a loss of pressure or by nasal congestion that is refractory to medical therapy. In those situations, a mask that covers both the nose and the mouth can be helpful.

2.5.2.2 Oral Appliances

Several studies have demonstrated that an oral appliance can be a useful alternative to positive airway pressure for some patients with sleep apnea. A wide variety of appliances are available, differing both in construction and in the manner in which they alter the oral cavity. Two of the more common oral appliances are shown in Fig 2.8. The appliances are worn only during sleep and are generally well tolerated. Not all patients have a clinically meaningful response to oral appliances, which are currently regarded as second-line therapy. Patients with mild sleep apnea who do not tolerate therapy with positive airway pressure are good

candidates for a trial of an oral appliance. Close collaboration between the physician and the dental consult-ant is necessary to ensure optimal patient selection and to avoid any alteration of dental occlusion or temporomandibular-joint discomfort.

Figure 2.4 Example of oral appliance

2.5.2.3 Medications

The use of medication to treat sleep apnea has been disappointing. Protriptyline and fluoxetine have been used with varying degrees of success in mild cases but are of little help in more severe cases. In patients with hypothyroidism, thyroxine replacement may significantly improve upper airway function during sleep. Nocturnal oxygen therapy is a possibility for patients who have severe desaturation and are intolerant of or will not accept other, more effective, treatments. Oxygen will decrease the nadir of oxyhemoglobin desaturation but its effect on the duration of apnea varies. There is no role for benzodiazepine sedative–hypnotic agents in patients with otherwise untreated sleep apnea. These medications will further destabilize the upper airway during sleep, impede arousal, and potentiate airway closure and oxyhemoglobin desaturation.

2.5.3 Surgical Treatments

2.5.3.1 Tracheostomy

The availability and acceptance of positive-pressure therapy have lessened the need for tracheostomy. There remains a small subgroup of patients with severe apnea who cannot tolerate positive pressure and for

whom other interventions are ineffective or unacceptable. A tracheostomy can provide dramatic improvement and be lifesaving, although additional medical and psycho-logical morbidity may be associated with this treatment.

2.5.3.2 Palatal Surgery

Surgery to modify, rather than bypass, a specific site of upper airway closure, although less disfiguring than tracheostomy, offers more variable results. The most commonly performed procedure, uvulopalatopharyngoplasty (LA-UPPP), is curative in less than 50 percent of patients. Preoperative imaging studies have not adequately predicted surgical success. Even when the technical results of surgery are good, obstruction may continue at the site of surgery in the soft palate, or elsewhere in the upper airway. Laser-assisted uvulopalatopharyngoplasty has recently been introduced as an outpatient treatment for snoring. This procedure is currently not recommended for the treatment of sleep apnea.

2.5.3.3 Maxillofacial Surgery

A variety of procedures have been developed to enhance upper airway patency during sleep in patients with obstruction at or below the base of the tongue. These procedures involve genioglossal advancement, with or without resuspension of the hyoid bone, and may be performed in conjunction with a uvulopalatopharyngoplasty. Such procedures usually require a team of surgeons that includes an otolaryngologist and an oral surgeon. These operations are not uniformly successful, although individual patients have had excellent results. Patients with sleep apnea who have major craniofacial abnormalities, or who have had an unsuccessful genioglossal advancement, with or without uvulopalatopharyngoplasty, may benefit from a maxillomandibular advancement (MMA). These procedures should be reserved for patients with sleep apnea who are either unwilling or un-able to be treated with positive airway pressure.

Chapter III

Computational Fluid dynamic

3. 1 Introduction

Computational fluid dynamics or CFD is the analysis of systems involving fluid flow, heat transfer and associated phenomena such as chemical reactions by means of computer-based simulation (14). In 1990s, CFD software has stepped into communication of industry owning to its adequately and economical complete.

With the widespread availability and powerful technique, CFD software broadly also used in many fields academics and research institutes. The unique advantage of CFD simulation over experimentation is ability to investigate the systems that unfeasible to perform. The precious information which is tough to be obtained in human analysis can be grant by virtual simulation. In field biomedical engineering, they allow various application of CFD such as blood flow prediction through an abnormal artery, drug delivery process in to the lungs of the pulmonary system simulation and modeling of particle dispersion from nasal sprayers and particle transport in nasal cavity. According to the non-invasive technique, the computational fluid dynamics analysis is applied in plenty researches in order to visualize the fluid flow characteristics in the upper airway such as velocity streamline, static wall pressure. Wall shear stress etc. (15-21).

There is three different approaches used for turbulence flow simulation, which is comprised of Reynolds-averaged Navier–Stokes (RANS) equations, Large Eddy Simulation (LES), and Direct numerical simulation (DNS). The number of respiratory flow researches in the past mainly focused on laminar flow because of limited resources and computational costs. For the past decades, turbulence model has been advocated in a variety of application areas. An example of CFD application using turbulence model with sleep apnea is Y. Fan et al. (20), study. They examined CFD analysis employed k - ε turbulence model on a specific OSA patient.

Computational fluid dynamics codes consist of three main processes as follow

3.1.1 pre-processing

This step consists of determine the geometry or computational model and generate meshed model.

3.1.2 Processing or solving setting

In this process including select the appropriate numerical method algorithm, defined material properties, boundary conditions, and initial conditions of solver.

3.1.3 Post-processing

When solving is done, we can all visualize, validate, and improve the results. The results can be illustrated in a variety of engineering physics. It also can be depicted the qualitative data such as velocity, pressure, momentum and temperature.

Then CFD processes can be summarized in Fig 3.1.

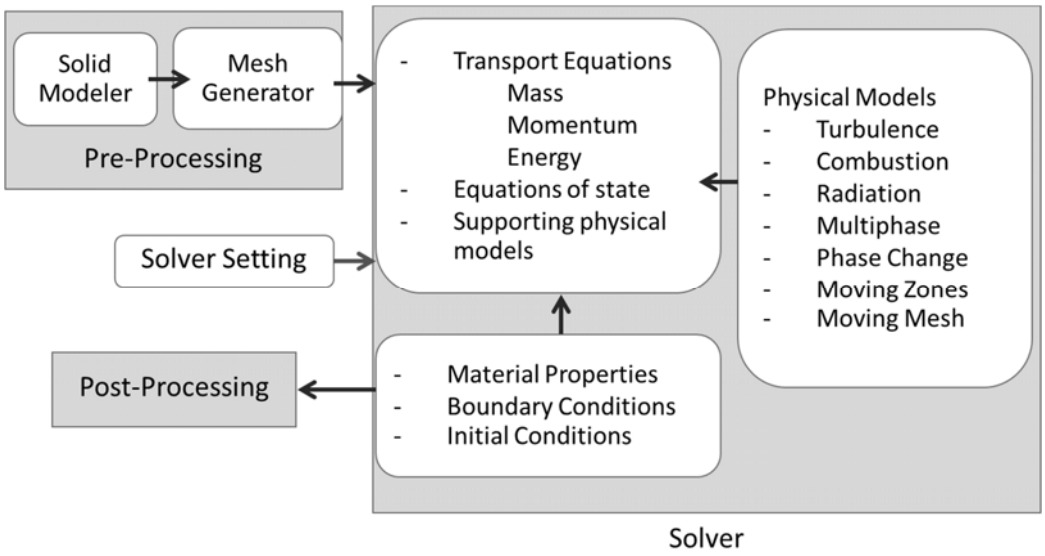

Figure 3.1 A CFD overview (39)

Aforementioned, Computational Fluid Dynamic technique has been performed in a wide range of biomedical applications which is emphasized in obstructive sleep apnea publications. This tremendous development of engineering simulation lead to the better outcome and superior surgical-assist tool in the near future. All necessary theories are provided in this chapter including governing equations of fluid flow, Navier-Strokes equations, and k - ε turbulence model. A brief summary of the finite volume method is stated in this chapter as well.

3. 2 Governing equations of fluid flow

The physical aspects of any fluid flow are based on the three fundamental principles-conservation of mass, momentum and energy (14). The Mathematical basis, which can be expressed their most general forms to integral and partial differential equations either, are elucidated for these fundamental physical principles.

The governing equations include the following conservation laws of physics:

3.2.1 The net rate of mass in the fluid element is conserved.

3.2.2 Newton's second law: the rate of change of momentum equals the sum of forces on a fluid particle

3.2.3 First law of thermodynamics (conservation of energy): rate of change of energy equals the sum of rate of heat addition to and work done on fluid particle.

The fluid will be regarded as a continuum. We describe the behavior of the fluid in terms of macroscopic properties, such as velocity, pressure, density and temperature, and their space and time derivatives. We consider such a small element of fluid with sides δ_x, δ_y and δ_z (Fig 3.2).

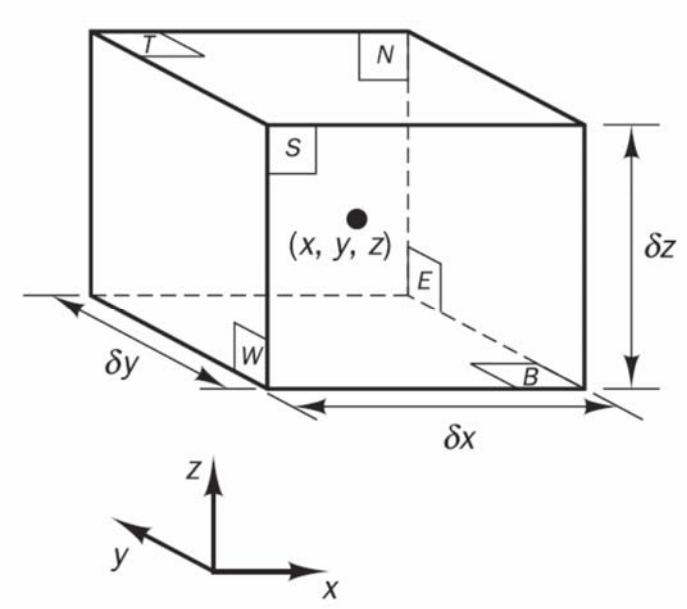

Figure 3.2 Fluid element for conservation laws (14)

The six faces are labeled N, S, E, W, T and B, which stands for North, South, East, West, Top and Bottom. The positive directions along the coordinate axes are also given. The center of the element is located at position (x, y, z). All fluid properties are

functions of space and time so we would strictly need to write ρ *(x, y, z, t)*, *p(x, y, z, t)*, *T(x, y, z, t)* and **u***(x, y, z, t)* for the density, pressure, temperature and the velocity vector respectively.

3.2.1 Mass conservation in three dimensions (continuity equation)

The physical principle of mass conservation is that mass is neither created nor destroyed. The first step in the derivation of the mass conservation equation is to write down a mass balance for the fluid element:

Rate of increase of mass in fluid element = Net rate of flow of mass into fluid element

The rate of increase of mass in the fluid element is

$$\frac{\partial}{\partial t}(\rho \delta x \delta y \delta z) = \frac{\partial \rho}{\partial t} \delta x \delta y \delta z \tag{3.1}$$

Where ρ is density, (*u, v, w)* are velocity in x, y, z direction respectively, and (δx, δy, δz) are sides of the element in x, y, x direction respectively.

Next we need to account for the mass flow rate across a face of the element, which is given by the product of density, area and the velocity component normal to the face. From figure 3.2, it can be seen that the net rate of flow of mass into the element across its boundaries is conserved. The rate of increase of mass inside the element (3.1) is now equated to the net rate of flow of mass into the element across its faces. All terms of the resulting mass balance are arranged on the left hand side of the equals sign and the expression is divided by the element volume $\delta x \delta y \delta z$. This yields

$$\frac{\partial \rho}{\partial t} + \frac{\partial (\rho u)}{\partial x} + \frac{\partial (\rho v)}{\partial y} + \frac{\partial (\rho w)}{\partial z} = 0 \tag{3.2}$$

or in more compact vector notation

$$\frac{\partial \rho}{\partial t} + \mathrm{div}(\rho \mathbf{u}) = 0 \tag{3.3}$$

Equation (3.3) is the unsteady, three-dimensional mass conservation or continuity equation at a point in a compressible fluid. The first term on the left

hand side is the rate of change in time of the density (mass per unit volume). The second term describes the net flow of mass out of the element across its boundaries and is called the convective term.

For an incompressible fluid, the density (ρ) is constant and equation (3.3) becomes

$$\text{div } \mathbf{u} = 0 \tag{3.4}$$

or in longhand notation

$$\frac{\partial u}{\partial x} + \frac{\partial v}{\partial y} + \frac{\partial w}{\partial z} = 0 \tag{3.5}$$

3.2.2 Momentum equation in three dimensions

The Physical principle of momentum equation (Newton's second law) is that the rate of change of momentum equals the sum of the forces on the particle:

Rate of increase of momentum of fluid = Sum of forces on fluid particle

The rates of increase of x-, y- and z-momentum per unit volume of a fluid particle are given by

$$\rho\frac{Du}{Dt} \qquad \rho\frac{Dv}{Dt} \qquad \rho\frac{Dw}{Dt} \tag{3.6}$$

It is common practice to highlight the contributions due to the surface forces as separate terms in the momentum equation and to include the effects of body forces as source terms.

The state of stress of a fluid element is defined in terms of the pressure and the nine viscous stress components shown in Fig 3.3. The pressure, a normal stress, is denoted by p. Viscous stresses are denoted by τ. The usual suffix notation τ_{ij} is applied to indicate the direction of the viscous stresses. The suffices *i* and *j* in τ_{ij} indicate that the stress component acts in the j-direction on a surface normal to the *i*-direction.

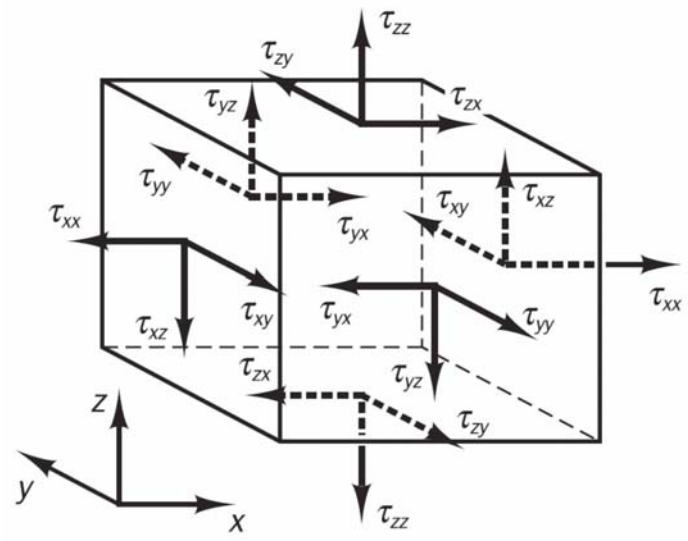

Figure 3.3 Stress components on three faces of fluid element (14)

Without considering the body forces in further detail their overall effect can be included by defining a source S_{Mx} of x-momentum per unit volume per unit time.

The x-component of the momentum equation is found by setting the rate of change of x-momentum of the fluid particle (3.6) equal to the total force in the x-direction on the element due to surface stresses plus the rate of increase of x-momentum due to sources:

$$\rho\frac{Du}{Dt}=\frac{\partial(-p+\tau_{xx})}{\partial x}+\frac{\partial\tau_{yx}}{\partial y}+\frac{\partial\tau_{zx}}{\partial z}+S_{Mx} \tag{3.7a}$$

the y-component of the momentum equation is given by

$$\rho\frac{Dv}{Dt}=\frac{\partial\tau_{xy}}{\partial x}+\frac{\partial(-p+\tau_{yy})}{\partial y}+\frac{\partial\tau_{zy}}{\partial z}+S_{My} \tag{3.7b}$$

the z-component of the momentum equation by

$$\rho\frac{Dw}{Dt}=\frac{\partial\tau_{xz}}{\partial x}+\frac{\partial\tau_{yz}}{\partial y}+\frac{\partial(-p+\tau_{zz})}{\partial z}+S_{Mz} \tag{3.7c}$$

The sign associated with the pressure is opposite to that associated with the normal viscous stress, because the usual sign convention takes a tensile

stress to be the positive normal stress so that the pressure, which is by definition a compressive normal stress, has a minus sign.

The effects of surface stresses are accounted for explicitly; the source terms S_{Mx}, S_{My} and S_{Mz} in (3.7a-c) include contributions due to body forces only. For example, we note that the body force due to gravity would be modeled by $S_{Mx} = 0$, $S_{My} = 0$ and $S_{Mz} = -\rho g$.

3.2.3 Energy equation in three dimensions

The energy equation is derived from the first law of thermodynamics, which states that the rate of change of energy of a fluid particle is equal to the rate of heat addition to the fluid particle plus the rate of work done on the particle:

Rate of increase of energy of fluid particle	=	Net rate of heat added to fluid particle	+	Net rate of work done on fluid particle

As before, we will be deriving an equation for the rate of increase of energy of a fluid particle per unit volume, which is given by

$$\rho \frac{DE}{Dt} \tag{3.8}$$

The total rate of work done on the fluid particle by surface stresses:

$$[-\mathrm{div}(p\mathbf{u})] + \left[\frac{\partial(u\tau_{xx})}{\partial x} + \frac{\partial(u\tau_{yx})}{\partial y} + \frac{\partial(u\tau_{zx})}{\partial z} + \frac{\partial(v\tau_{xy})}{\partial x} + \frac{\partial(v\tau_{yy})}{\partial y} + \frac{\partial(v\tau_{zy})}{\partial z} + \frac{\partial(w\tau_{xz})}{\partial x} + \frac{\partial(w\tau_{yz})}{\partial y} + \frac{\partial(w\tau_{zz})}{\partial z} \right] \tag{3.9}$$

The rate of heat addition to the fluid particle due to heat conduction across element boundaries:

$$-\mathrm{div}\ \mathbf{q} = \mathrm{div}(k\ \mathrm{grad}\ T) \tag{3.10}$$

Here, q is the heat flux vector, k is conductive heat transfer coefficient, T is temperature, and S_E is a source of energy per unit volume per unit time.

In addition, the energy equation defined as:

$$\rho\frac{DE}{Dt} = -\mathrm{div}(p\mathbf{u}) + \left[\frac{\partial(u\tau_{xx})}{\partial x} + \frac{\partial(u\tau_{yx})}{\partial y} + \frac{\partial(u\tau_{zx})}{\partial z} + \frac{\partial(v\tau_{xy})}{\partial x} + \frac{\partial(v\tau_{yy})}{\partial y} + \frac{\partial(v\tau_{zy})}{\partial z} + \frac{\partial(w\tau_{xz})}{\partial x} + \frac{\partial(w\tau_{yz})}{\partial y} + \frac{\partial(w\tau_{zz})}{\partial z}\right] + \mathrm{div}(k\ \mathrm{grad}\ T) + S_E \quad (3.11)$$

3. 3 Navier-Stokes Equations

The governing equations we describe employ to inviscid-incompressible flow for steady state. Although, Inviscid flow analyses are suitable of high-Reynolds number applications, This may be the only way to obtain the calculation initiated in such a complicated flow like human airflow (39). Additionally, assuming the flow incompressibility because of very low Mach number (<<0.3) (19). Applying the mass, momentum and energy conservation, we can simplify the Navier-Strokes equations in the most useful form for the development of finite volume method as follow:

$$\rho\frac{Du}{Dt} = -\frac{\partial p}{\partial x} + \mathrm{div}(\mu\ \mathrm{grad}\ u) + S_{Mx}$$

$$\rho\frac{Dv}{Dt} = -\frac{\partial p}{\partial y} + \mathrm{div}(\mu\ \mathrm{grad}\ v) + S_{My}$$

$$\rho\frac{Dw}{Dt} = -\frac{\partial p}{\partial z} + \mathrm{div}(\mu\ \mathrm{grad}\ w) + S_{Mz} \quad (3.12)$$

Noted that ρ is density, (*u, v, w)* are velocity in x, y, z direction respectively, p is pressure, and (S_{Mx}, S_{My}, S_{Mz}) are the source terms of x, y, z momentum respectively.

.

3. 4 k - ε turbulence model

The k - ε model was developed to by Launder and Spalding in 1974 (40). It is one of the most common turbulence model employed in CFD simulation (14). It is a two equation model which gives a general dissipation of turbulence by means of two transport equation (PDE's)

For turbulence energy (k) has its own transport equation:

$$\frac{\partial(\rho k)}{\partial t} + \mathrm{div}(\rho k \mathbf{U}) = \mathrm{div}\left[\frac{\mu_t}{\sigma_k}\,\mathrm{grad}\ k\right] + 2\mu_t S_{ij} \,.\, S_{ij} - \rho\varepsilon \tag{3.13}$$

For dissipation rate (ε) which is entirely modeled phenomenologically as follows:

$$\frac{\partial(\rho\varepsilon)}{\partial t} + \mathrm{div}(\rho\varepsilon \mathbf{U}) = \mathrm{div}\left[\frac{\mu_t}{\sigma_\varepsilon}\,\mathrm{grad}\ \varepsilon\right] + C_{1\varepsilon}\frac{\varepsilon}{k}2\mu_t S_{ij} \,.\, S_{ij} - C_{2\varepsilon}\rho\frac{\varepsilon^2}{k} \tag{3.14}$$

Dimensionally, we use k and ε to define velocity scale (ϑ) and length scale (ℓ) representative of the large-scale turbulence as follows:

$$\vartheta = k^{1/2} \quad \ell = \frac{k^{3/2}}{\varepsilon} \tag{3.15}$$

Together with the k equation, eddy viscosity can be expressed as:

$$\mu_t = C\rho\vartheta\ell = \rho C_\mu \frac{k^2}{\varepsilon} \tag{3.16}$$

Where C_μ is a dimensionless constant. The standard k - ε model employs values for the constants that are arrived at by comprehensive data fitting for a wide range of turbulent flows:

$$C_\mu = 0.09 \quad \sigma_k = 1.00 \quad \sigma_\varepsilon = 1.30 \quad C_{1\varepsilon} = 1.44 \quad C_{2\varepsilon} = 1.92$$

3. 5 Finite Volume Method

The finite volume method (FVM), a discretization method, has been applied with a variety type of numerical simulation (i.e. elliptical, parabolic or hyperbolic equations) which is conservation law (41). FVM, in fact, is developed from finite difference method. Plenty field of engineering researches such as fluid flow; heat and mass transfer employ this method. Domain of FVM is written on each discretization cell known as control volume; by the divergence formula, which is an integral formulation of the fluxes over the boundary of control volume is then achieved (Fig 3.4). The fluxes on the boundary are discretized with respect to the unknown of discrete.

The finite volume method has likewise characterized the finite element method (FEM) (42). Both, for example, can be used on arbitrary geometries and applying unstructured or structured meshes, and it leads to robust schemes. However, when the flux is so significant in such fluid mechanic problems, FVM has been performed more than FEM because of locally conservation on control volume.

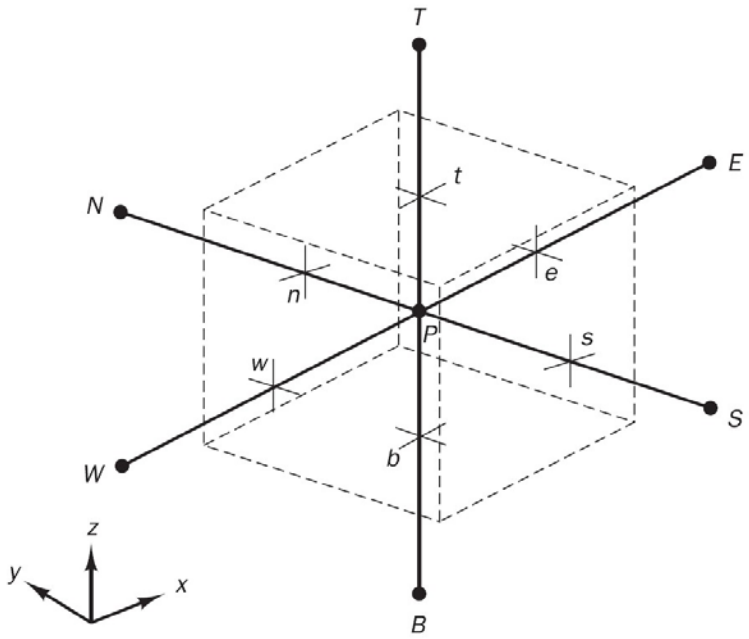

Figure 3.4 Definition of control volume, a cell in three dimensions and neighbouring nodes (42)

A cell containing node P now has six neighbouring nodes identified as west, east, south, north, bottom and top (*W, E, S, N, B, T*). As before, the notation *w, e, s, n, b* and *t* is used to refer to the west, east, south, north, bottom and top cell faces respectively.

CHAPTER IV

Experimental Methods

4. 1 Introductions

In this chapter, the experimental methods for performing a research analysis are outlined below in Fig 4.1, so as to provide a reference for understanding the various steps.

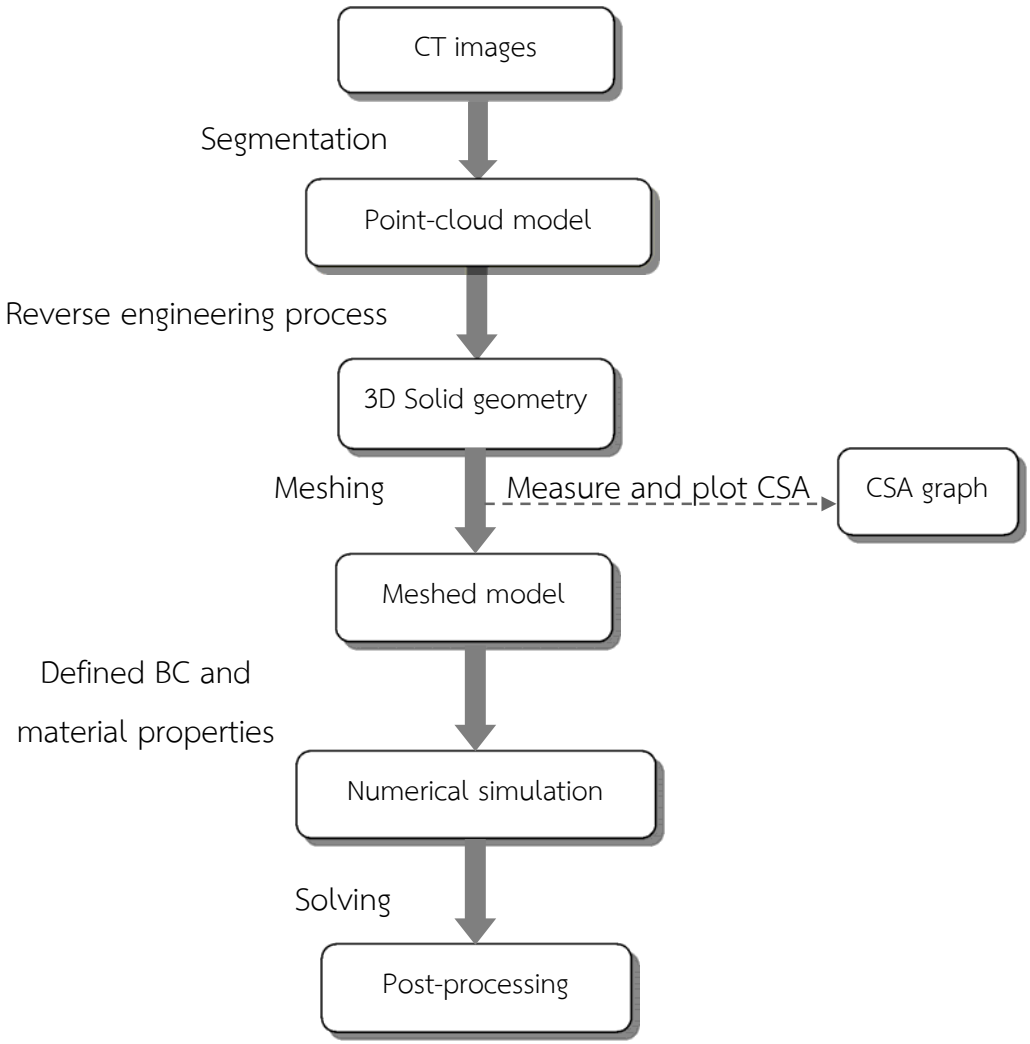

Figure 4.1 Steps for CFD simulation

The figure above gives series of the step that would be involved in this analysis. To understanding the CFD simulation in OSA, data acquisition of CT scan is noted in section 4.2 initially. Modeling the airway-structure by mean of segmentation will be described in section 4.3. The outcome geometry, which called point-cloud model, reverse engineering process is considered in section 4.4 for building up a 3D solid geometry and simplification it. How to obtain the cross-sectional area for comparison OSA patient and healthy subjects is then explained in section 4.5. With these models have built up, we actually segregated it into smaller fragments known as mesh will be clarified in section 4.6. Since a finite flow domain is specified, boundary and initial conditions are defined for the numerical simulation that would be presented in section 4.7. The last step will be detailed in section 4.8 is solution solving with finite volume solver and post- processing the obtained results.

4. 2 CT Data Acquisitions

Medical images play an important role in advanced medicine nowadays. Such Computed tomography (CT), illustrated a series of axial CT images in Fig 4.2, is an effective modality provides an anatomical human body with noninvasive techniques. Scientists and biomedical engineer also require physiological information of patient- specific structure to simulate the airflow dynamic. Especially in complex airway such human respiratory tract, assessment of geometric accuracy is essential. To obtaining satisfied results in this study, CT data could be grouped with CFD simulation in OSA.

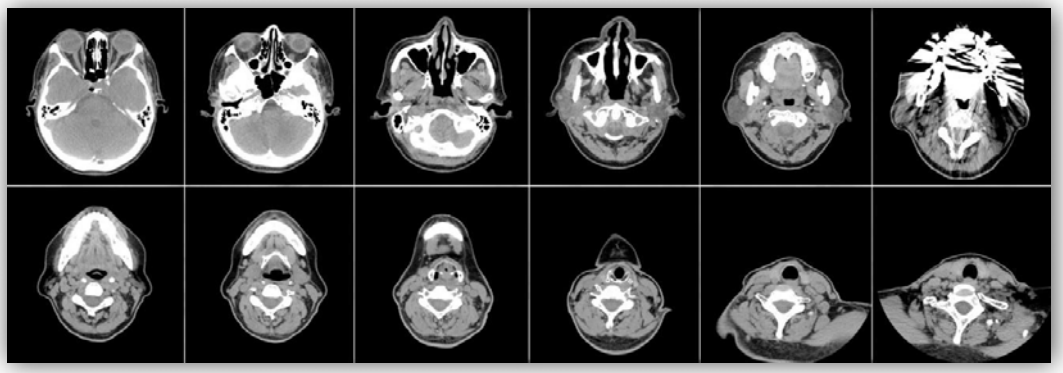

Figure 4.2 A set of CT slices in axial plane of a human upper airways

The airway models were constructed on a moderate-severe OSA patient, 43 years old, 26.81 kg/m^2-BMI, 12.9 times/hour-AHI, compared with three healthy subjects. All healthy subjects had normal respiratory functions and were selected from ENT department who underwent neck CT at an Imaging Storage Center of Advanced Diagnostic Imaging and Image-Guided Minimal Invasive Therapy Center (AIMC), Ramathibodi Hospital. CT data were obtained with an Aquilion ONE 320-Slice (TOSHIBA) at AIMC with the following parameters: 100 kVp, 150 mAs, 1 mm slice thickness. CT Scanning range from nostril through hypopharynx was collecting while subjects were either awaking or sleeping in supine position, perpendicular to table in Frankfort plane.

In order to determine OSA patient, polysomnography (PSG) is considered for diagnosis the apnea during sleep. Typically, PSG is conducted overnight recording the physiological changes including brain activity (EEG), eye movement (EOG), skeletal muscle activation (EMG), heart rate (ECG), oxygen saturation, oronasal airflow, as well as thoracic and abdominal movement. To carry out this test, the patient had to prepare himself by avoiding slumber and abstain from alcohol, caffeine, cigarettes, and exercise that could affect the sleep before examined date. Therefore, we took no longer than three hours to imitated nighttime sleepiness.

This procedure cooperated radiological and polysomnographic technicians. In essence, while polysomnogram was indicating patient's sleep state and decrease of blood oxygen, CT was starting scan. As you can see in Fig 4.3. CT images were then transformed directly via a DICOM format to mimic software which is dedicated to the analysis of medical imaging.

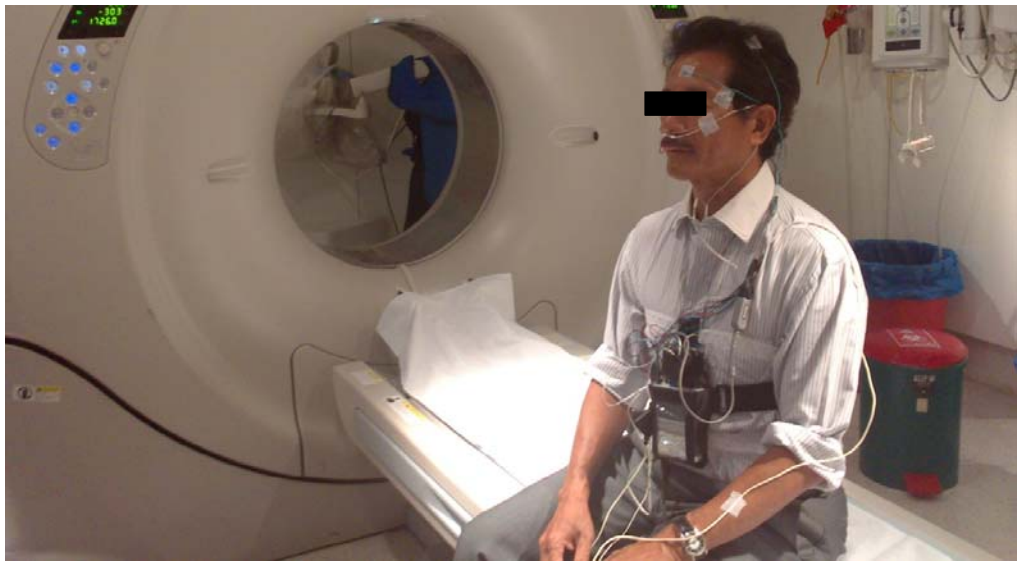

(a)

(b)

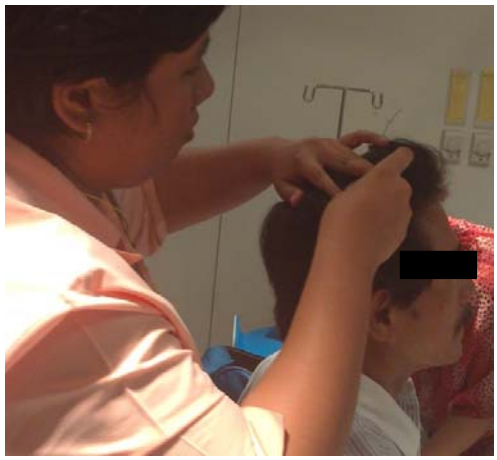

(d)

(c)

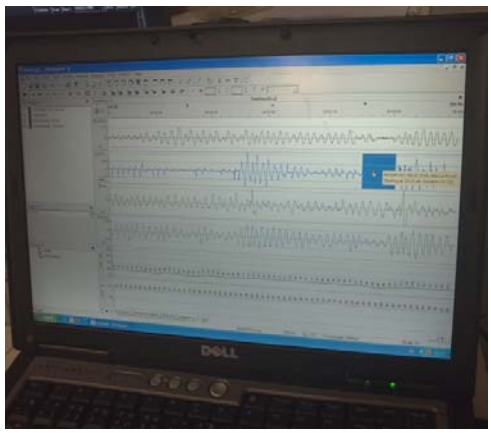

(e)

Figure 4.3 The process of combined CT images with PSA data, (a) subject with PSG test in scanning process, (b, c) radiological technician performed CT scan, and (d, e) PSG technician recorded sleep test

4. 3 Airways Structure-modeling

3D models were performed in MIMIC software, which was used for various operations of visualization, segmentation, registration, pre-filtering, and interpolation standardization of CT images. CT of all airways were segmented by semi-automated identification of airways followed by manual identification of seed pixels in selected slices.

Thresholding range from 1024 to -256 HU was selected initially to select the area of interest, from nostril to hypopharyx which is exclude paranasal sinuses and oral cavity as shown in Fig 4.4. Anatomical 3D raw models were generated for all subjects (OSA and healthy subjects) and were then exported in binary STL format for CFD model preprocessing. Figure 4.5 shows the surfaces rendition of the upper airway either of healthy subject and OSA patient in the mimic graphical user interface.

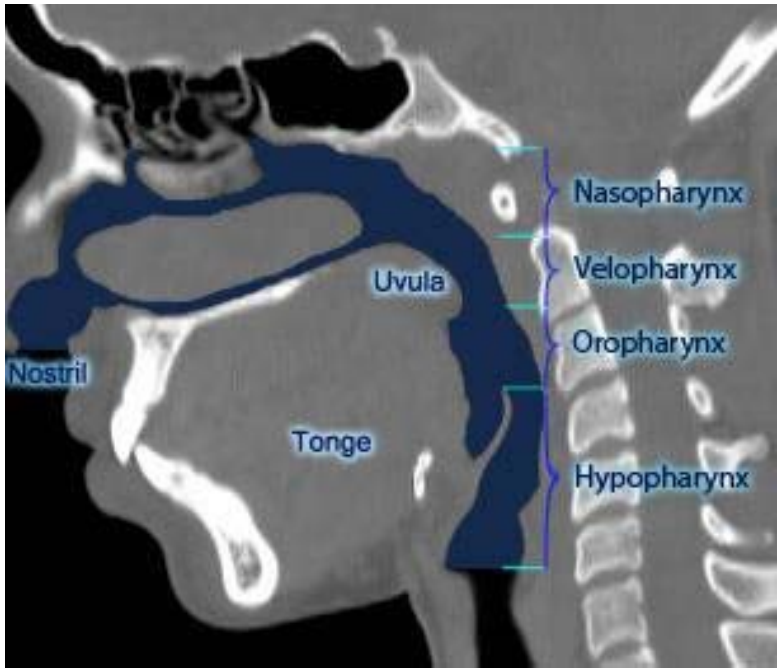

Figure 4.4 The region of interested, begin with nostril to hypopharynx through Upper airway

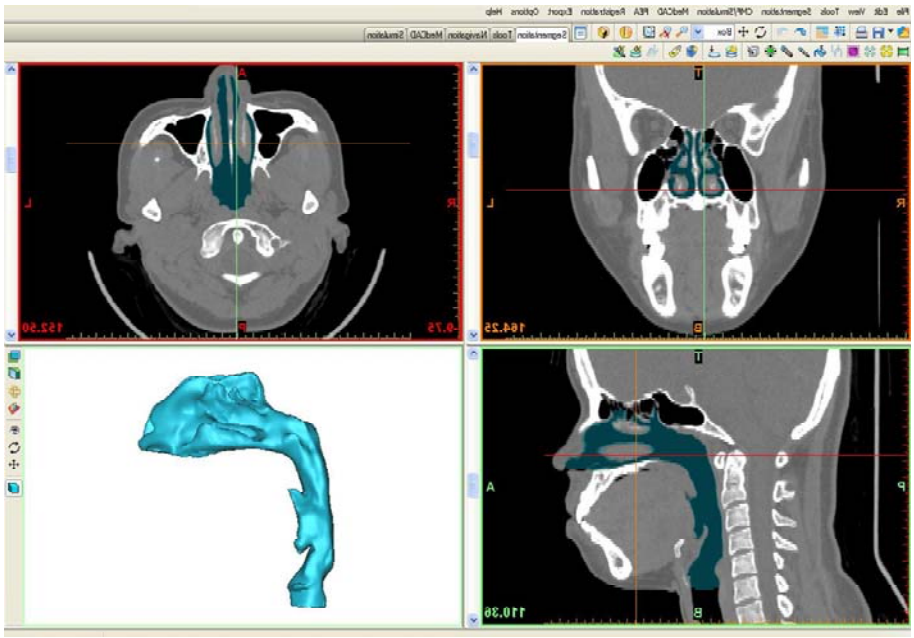

(a)

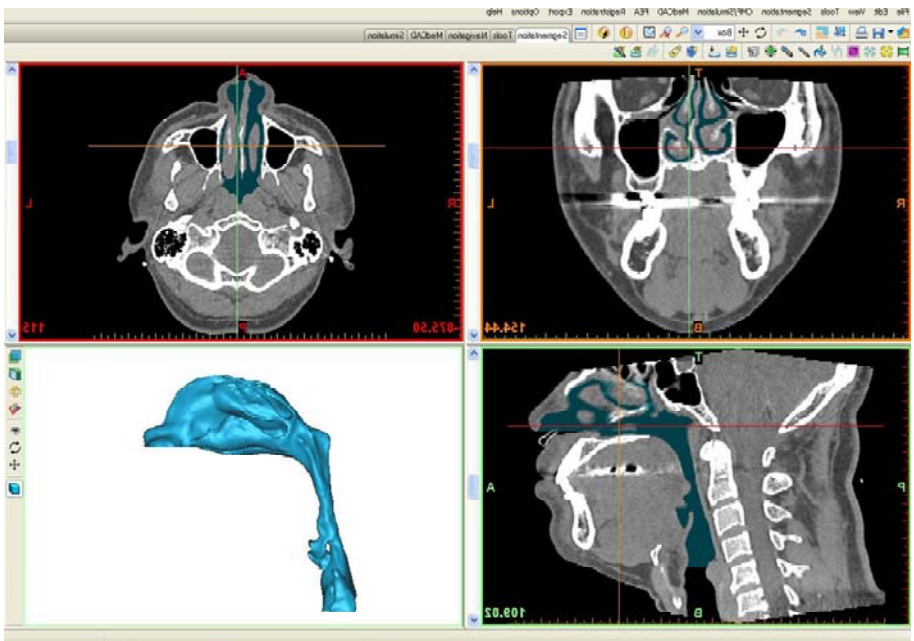

(b)

Figure 4.5 illustrated MIMIC GUI and point-cloud model (a) healthy subject and (b) patient associated with OSA

4. 4 Reverse Engineering Process

This techniques used to converse STL file format to be solid model in parasolid (x_t) file format by surface rendering. In additions, to overcome the difficulties in the meshing and numerical simulation afterwards, interactive image re-segmentation was perform using XOR to patch discontinuities with least loss of information per slice. And improve the surface quality by smoothing

Figure 4.6 and 4.7 demonstrate reverse engineering process in example of manufacture and solid model used in this study from commercial software which are similarity. Format of x_t, which is importable by commercial CFD software, were exported. Finally, the entire airway models were cut at nostril to be inlet faces and hypopharynx to be outlet face perpendicular to sagittal plane of each model.

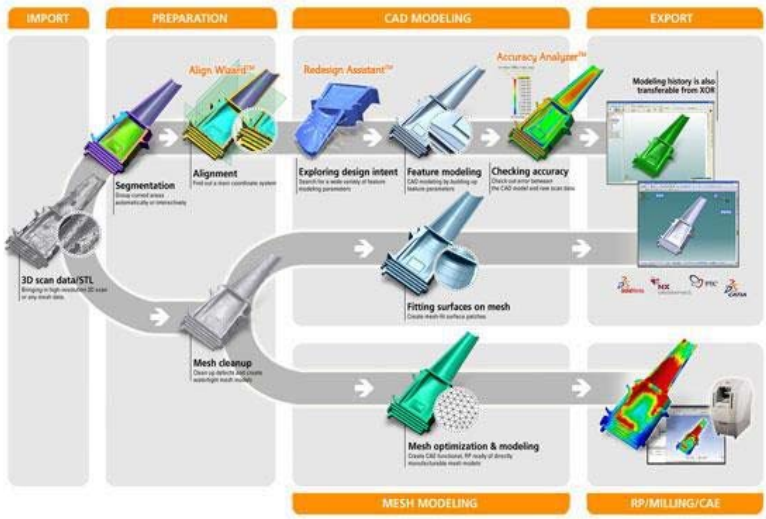

Figure 4.6 Manufacturing including reverse engineering process

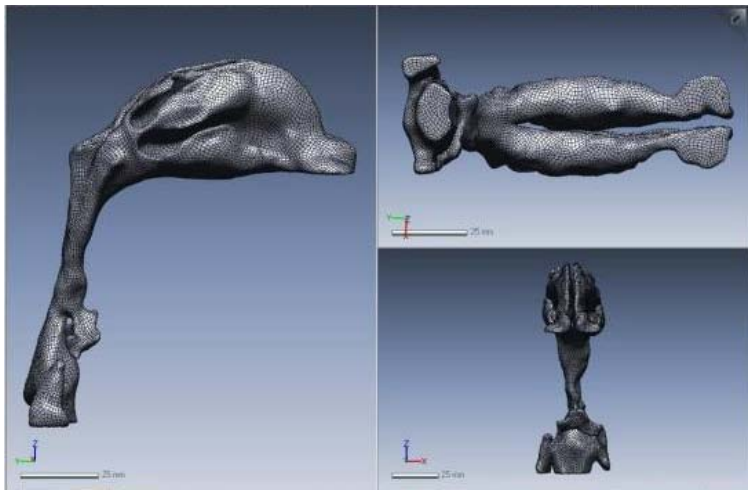

Figure 4.7 Solid model in commercial software

4. 5 Mesh Generations

For Mesh generation, commercial software ICEM-CFD (ANSYS) was employed to create instructed hybrid volume mesh. The smallest size was 0.3 mm and set to be 5 layers at the wall, so, total elements of either 3D model approximately range from 10,000,000 to 14,000,000 elements. Figure 4.8 exhibits the volume mesh and magnified viewing through the anterior tip of inferior turbinate.

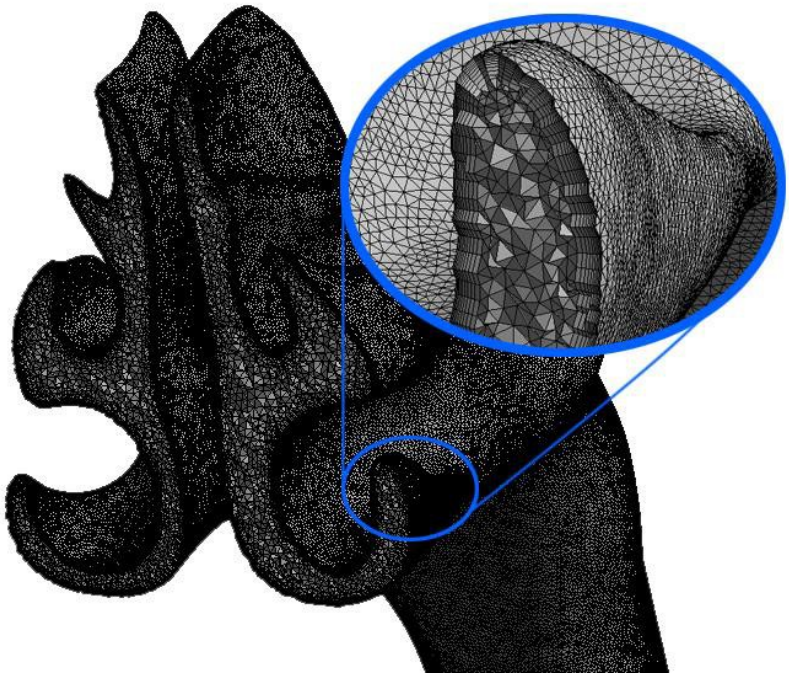

Figure 4.8 Volume mesh and cut plane

Table 4.1 Shown the properties of volume and mesh elements of all models

Model	Volume (mm^3)	Mesh Elements
Healthy1	43843	3195661
Healthy2	44006	3240769
Healthy3	39348	2946900
OSA	37787	12079666

4. 6 Numerical Simulations

CFD package software (FLUENT) was used in this research. The airflow was assumed to be incompressible and steady state. The boundary was located from nostrils as inlets to hypopharynx region as the outlet. The mass flow rate was 250 ml/s. The material properties of air are considered as follow software default properties, which is demonstrated in Fig 4.9.

```
((air
fluid
(chemical-formula . #f)
(density (constant . 1.225)
(premixed-combustion 1.225 300))
(specific-heat (constant . 1006.43))
(thermal-conductivity (constant . 0.0242))
(viscosity (constant . 1.7894e-05)
(sutherland 1.7894e-05 273.11 110.56)
(power-law 1.7894e-05 273.11 0.666))
(molecular-weight (constant . 28.966))
```

Figure 4.9 Material properties of air (39)

Additionally, the wall of airway was defined to be no-slip condition. The low Reynolds number k - ε turbulent model was employed for capture possible existences of turbulence. The pressure was set to be zero (Pa) at the outlet to mimic the normal breathing during inhalation, as shown in Fig 4.10. The compliance of the airway was neglected. Discretization of the governing equations were performed using a Semi Implicit Method for Pressure Linked Equations (SIMPLE) which widely used for manage pressure-velocity coupling and the Navier–Stokes equations were concerned in this simulation. We used computer: CPU – Intel i7 3610, 16 GB of RAM

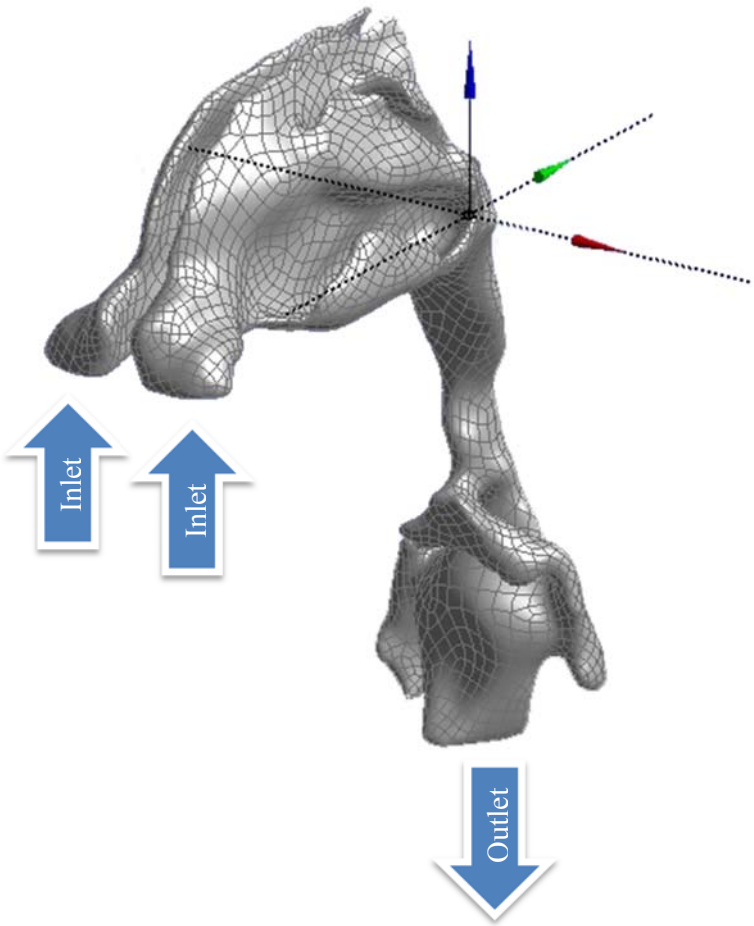

(a)

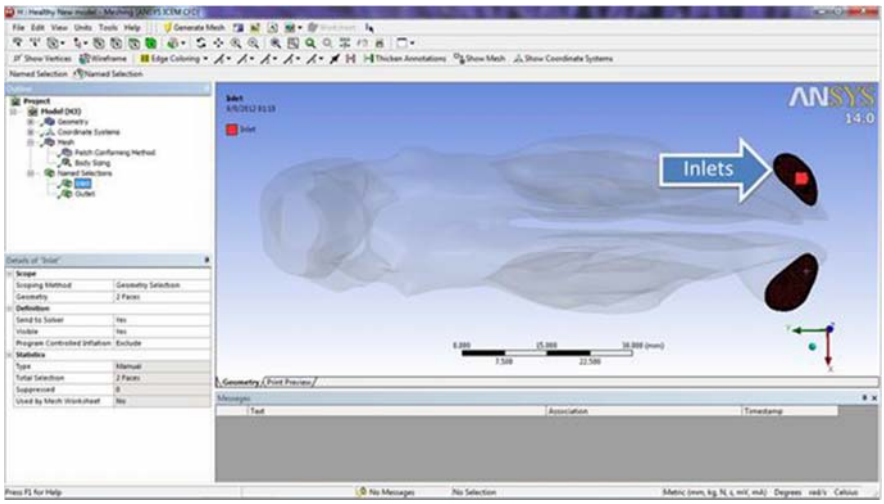

(b)

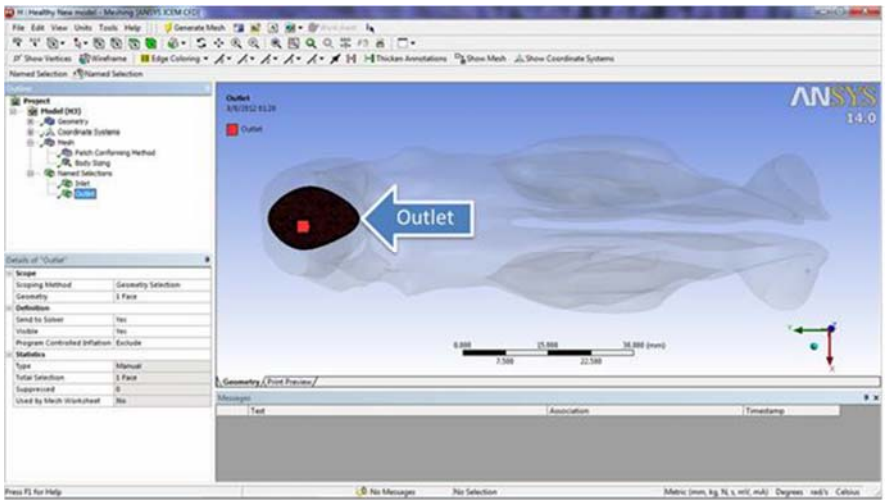

(c)

Figure 4.10 Boundary condition setting for airflow simulation in CFD commercial software, (a) Defined inlet and outlet boundary condition in 3D model, (b) inlet boundary at nostril, and (c) outlet boundary at velopharynx

4. 7 Post-Processing

In respect to comparative the airflow characteristics, CFD-Post package software (FLUENT) was employed. These simulation results of OSA model and three normal respiratory subjects are listed as follow:

- Velocity streamline (m/s)
- Pressure distribution (Pa)
- Wall Shear Stress (WSS)
- Cross-sectional areas (mm^2)
- Three-dimensional models

CHAPTER V

Results and Discussions

5. 1 Introductions

The achievements of this study lie in comparative computational fluid dynamic results of airflow characteristics between obstructive sleep apnea patient and three baseline healthy subjects. To analyze the airflow characteristics, cross-sectional area, velocity magnitude, pressure distribution, and wall shear stress during tidal breathing has been modeled in a Thai-OSA patient and three healthy subjects. Also, these parameters are investigated for supine postures in Frankfort plane as was mentioned in section 5.2.

The numerical simulation was conducted through k - ε turbulent model to assess results including velocity magnitude, pressure drop distribution, and wall shear stress. This study also explains the issue relating to cross-sectional area of human upper respiratory through from nostril to velopharynx. The results will be depicted as follow:

5. 2 Velocity streamline

Velocity streamline (m/s) is an essential parameter extracted from computational fluid dynamics. All of velocity contours for each model at mid sagittal plane was shown in Fig. 5.1 and plotted in Fig. 5.2, indicated maximum velocity at velopharynx which usually is the narrowest also.

5. 3 Pressure distribution

The Distribution of pressure is the next characteristic extracted from airflow simulation. Pressure gradient was exhibited in Fig. 5.3 in mid sagittal plane and also displayed for comparison along inlet pressure with negative pressure drop of obstructive model and positive pressure gradient of baseline models. Figure 5.4 demonstrated significant pressure distribution among Healthy and OSA patient. Moreover, the gradient of pressure is similar to velocity as mentioned before.

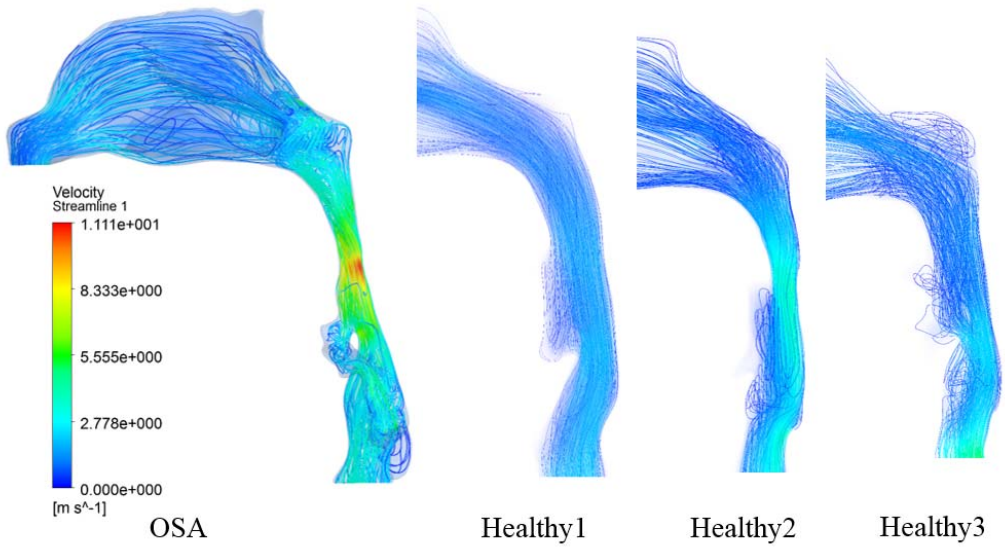

Figure 5.1 Illustrated contour plot of velocity streamline of all subjects at mid sagittal plane; patient associated with OSA, Healthy1, Healthy2, and Healthy3, respectively

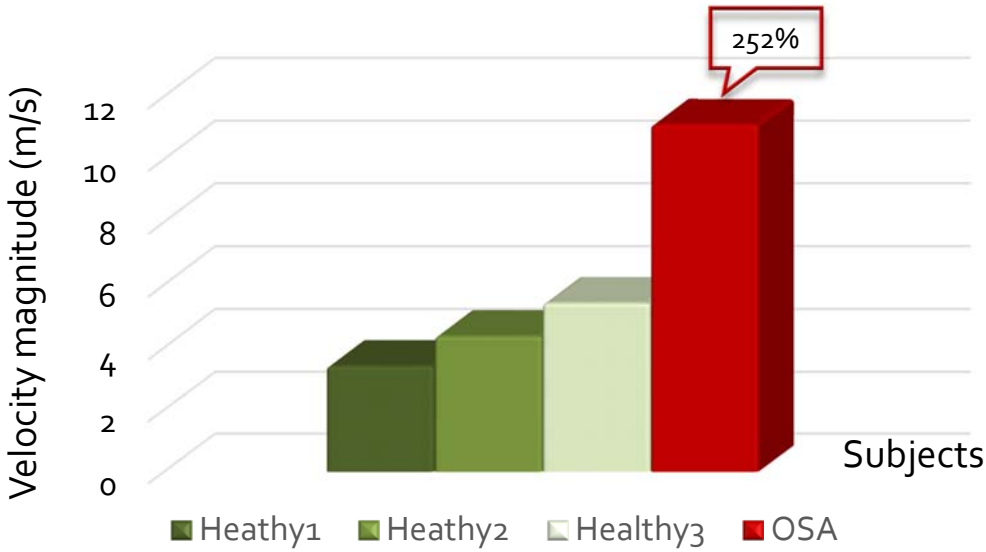

Figure 5.2 shown maximum velocity magnitude (m/s) at constricted area of entire models

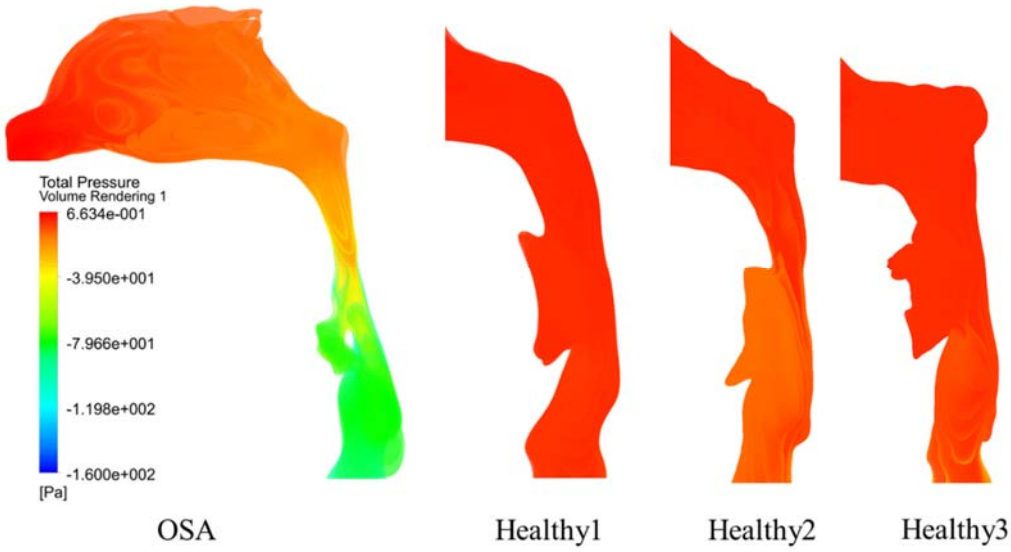

Figure 5.3 Indicated pressure gradients of inspired flow among subjects at mid sagittal plane; patient associated with OSA, Healthy1, Healthy2, and Healthy3, respectively

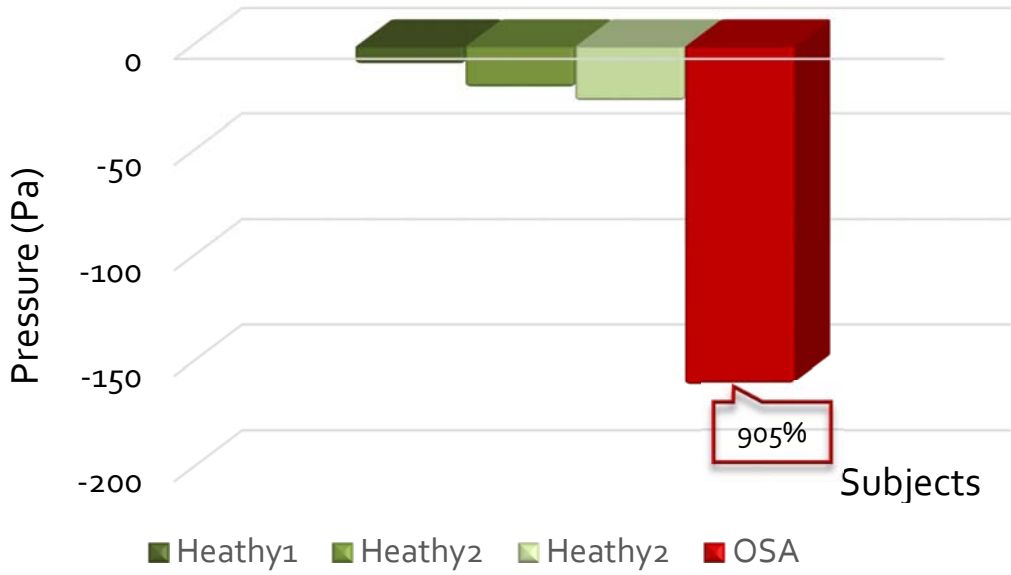

Figure 5.4 Comparative significant pressure distribution results from CFD at narrowed region (a) Healthy1, (b) Health2, (c) Healthy3, and (d) patient associated with OSA

5. 4 Wall shear stress

Because respiration in upper human area has effected by plenty of factors, the outcome of increase inspired airflow should be examined as well. Shear stresses at respiratory wall is one of important parameters should be concerned. Wall Shear Stress (WSS) was investigated then illustrated as 3D contours in Fig. 5.5 and plotted in Fig 5.6.

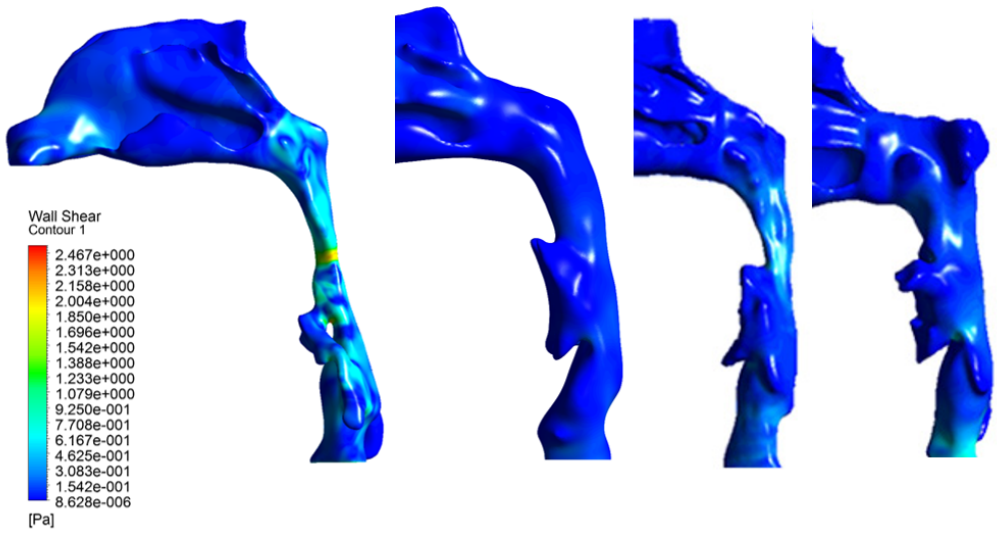

Figure 5.5 Presented wall shear stress contours in each geometry; patient associated with OSA, Healthy1, Healthy2, and Healthy3, respectively

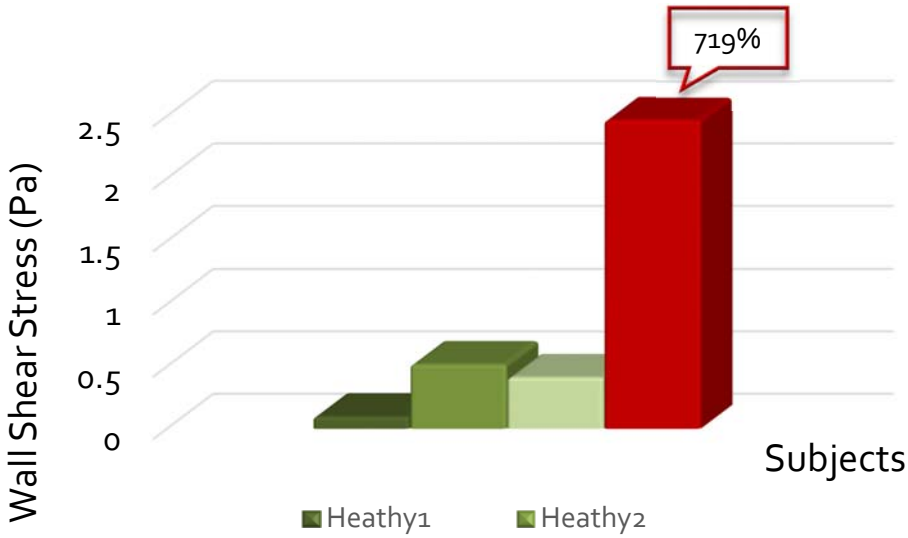

Figure 5.6 Reveal maximum WSS among models (a) Healthy1, (b) Health2, (c) Healthy3, and (d) patient associated with OSA

5. 5 Cross-sectional area

Sleep apnea is a sleep disorder characterized by abnormal pauses in breathing or instances of abnormally low breathing, during sleep. Thy why cross-sectional area should be concerned regard as respiratory constriction threatened to patient's life. The airway areas in axial planes were measured from three dimensional models. Since there had a lot of discrepancy in geometry, this study validated them in the narrowest portion which was located as #0 position. Then, they were further divided by 1 millimeter upper and lower location which was shown in negative and positive sign respectively. The results exhibited that CSA of OSA patient had the narrowest area was 9.304 mm^2. Meanwhile CSA of healthy#1, #2, and #3 was 68.404, 120.970, and 44.980 mm^2 consequently as shown in Table 5.1 that was shown issue relation of cross-sectional area in each position among geometry. In addition, relationship between CSA (mm^2) and slide position (#) was graphically described in Fig 6.10.

Table 5.1 Cross-sectional areas were measured in different axial plane divided by 1 mm which slide position (#) 0 is the constrictive region of all airway geometries

Slide position (#)	*CSA (mm^2)*			
	Health1	Healthy2	Healthy3	OSA
-20	602.738	231.232	254.8745	351.708
-19	433.7275	193.772	259.4136	298.67
-18	337.0507	170.198	262.2668	255.776
-17	302.8776	154.77	265.5291	223.266
-16	284.0663	143.957	298.077	196.671
-15	271.7007	136.58	326.3802	173.247
-14	262.6232	130.747	366.1685	152.977
-13	255.0654	125.886	364.9897	136.176
-12	247.9999	120.67	344.9099	120.642
-11	240.7766	115.275	330.5678	104.869
-10	232.8694	110.455	312.2522	89.832
-9	224.0824	106.17	296.5352	75.619
-8	214.546	102.203	283.0914	62.625
-7	204.8062	98.291	248.1021	49.691
-6	195.3122	94.148	231.1941	38.617
-5	186.3786	89.528	225.555	30.907
-4	178.1164	84.714	235.1862	24.383
-3	170.9356	79.689	245.6907	18.377
-2	164.8369	74.632	228.3784	13.898
-1	160.3739	70.289	210.2001	10.896
0	158.6996	68.404	117.6358	9.304
1	161.5787	99.604	126.1204	9.385

Table 5.1 Cross-sectional areas were measured in different axial plane divided by 1 mm which slide position (#) 0 is the constrictive region of all airway geometries (continuous)

Slide position (#)	*CSA (mm^2)*			
	Health1	Healthy2	Healthy3	OSA
2	193.4226	128.592	140.2943	10.474
3	212.1204	152.379	157.6752	13.054
4	225.3184	172.887	176.6498	16.048
5	237.8267	193.699	195.0671	19.1
6	250.3565	212.026	210.7206	21.453
7	262.8358	228.269	222.6655	23.295
8	274.8998	244.123	230.1845	25.226
9	285.0199	258.4	232.3241	29.021
10	292.5852	269.258	219.4364	36.712
11	297.6134	275.83	210.3631	46.42
12	300.7022	279.082	192.7582	57.241
13	302.8634	278.435	177.397	68.812
14	304.6466	272.567	163.2089	81.323
15	305.6916	265.875	149.8491	95.748
16	305.2411	259.242	137.5002	110.461
17	303.5587	259.844	126.1373	124.764
18	301.1666	265.779	114.8041	139.654
19	298.4053	269.938	102.6156	154.762
20	294.4256	268.019	89.66272	170.357

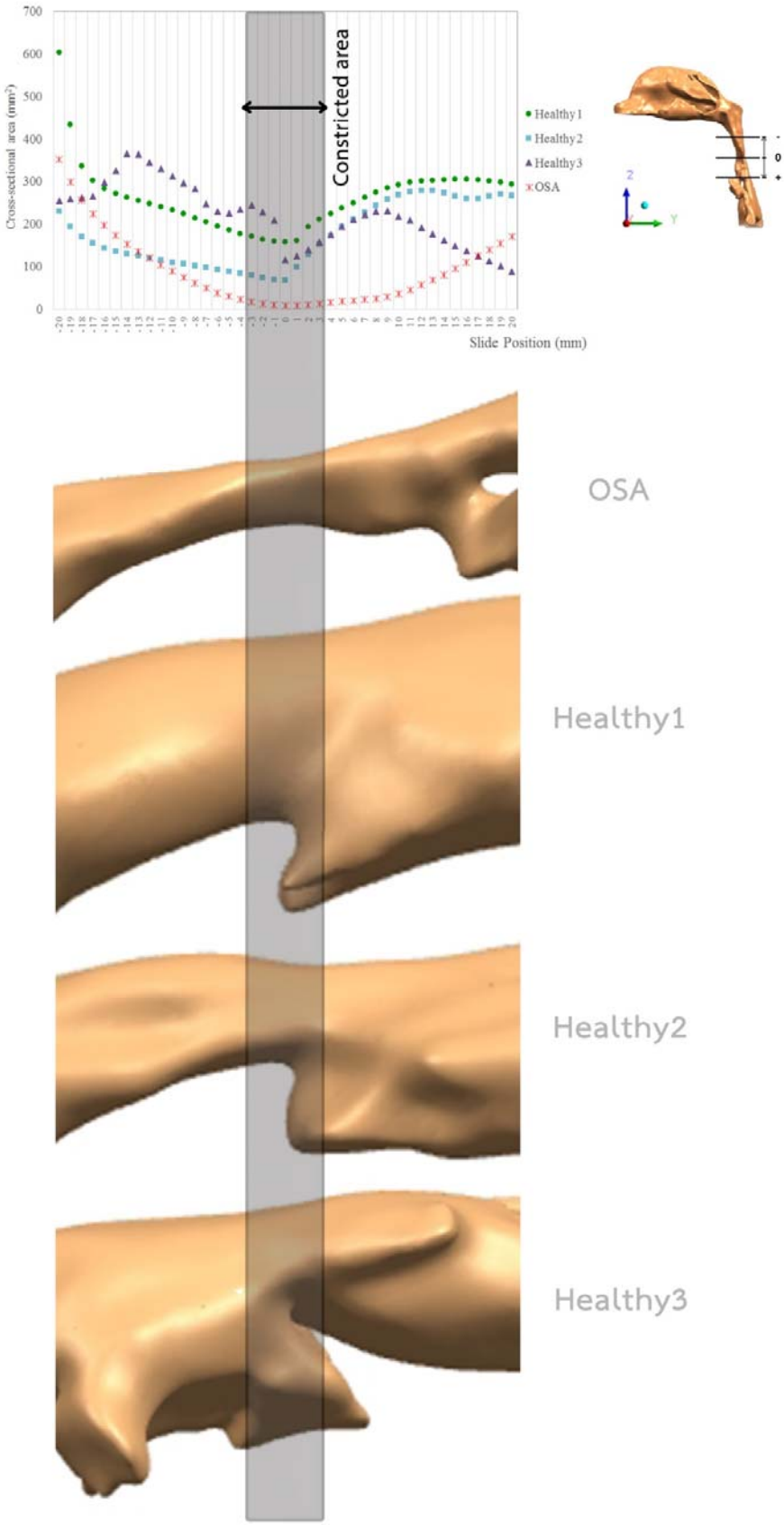
Cross-sectional area (mm²)
Slide Position (mm)
Constricted area
Healthy 1
Healthy 2
Healthy 3
OSA
OSA
Healthy1
Healthy2
Healthy3

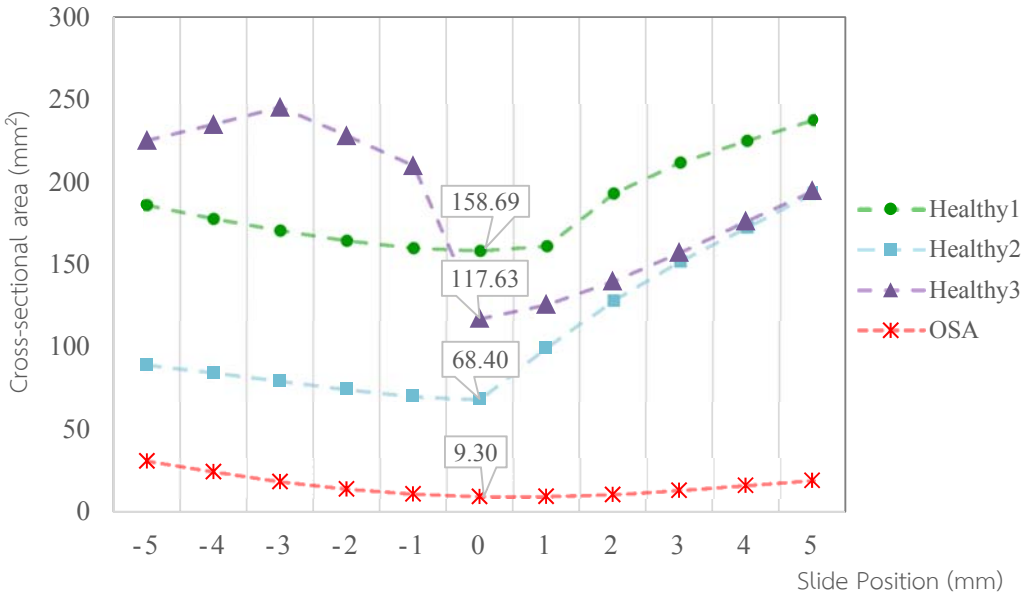

Figure 5.7 Plotted cross-sectional areas (CSA) with slide position among OSA and three healthy airways in axial plans (upper picture) and Enlarge constricted region where the obstruction (lower picture) occur. Notice that #0 represents the narrowest region; #upper positions represents in negative signs; #lower positions represents in positive signs)

5. 6 3D geometry of OSA patient

We obtained information of upper respiratory tract following CT data acquisition first. Then, segmentation the region of interest and reconstruction the airway of OSA patient were conducted. The three-dimensional models were rendered after that. A summary processes from CT data acquisition to rendering 3D models are depicted in figure 5.8. Reminded that we was capturing CT images while physiological signals of polysomnogram indicated patient was sleeping compared with having airway obstruction. The left column performed while patient was sleeping and the right one focuses on occurring apnea.

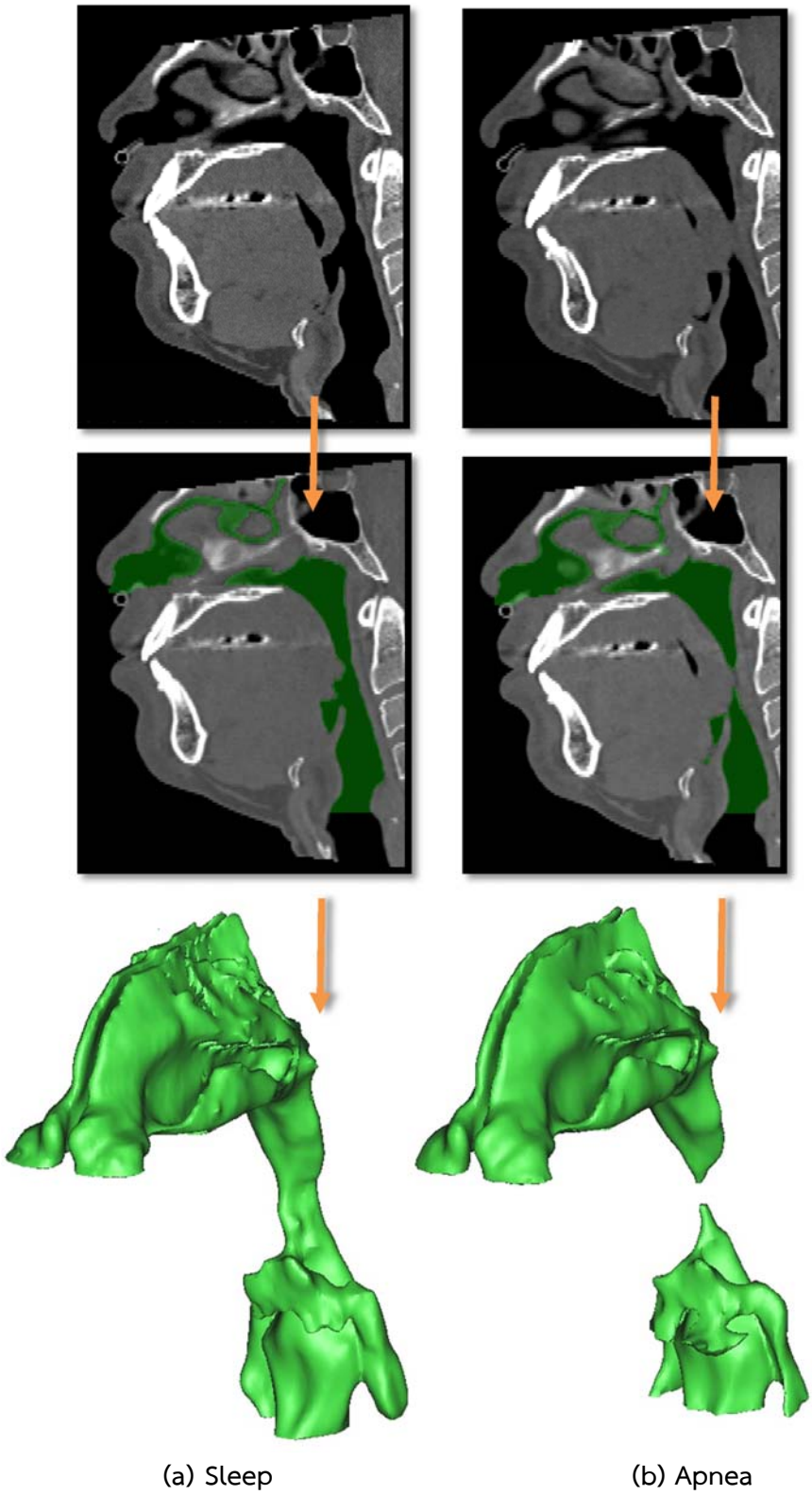

Figure 5.8 Three-dimensional airway geometry of patient who having OSA reconstructed from CT images during (a) sleep and (b) apnea

5. 7 Discussions

This study focuses on applied Computational Fluid Dynamics (CFD) with Obstructive Sleep Apnea (OSA) base on Computed Tomography (CT) images to investigate flow characteristics in upper airway. OSA has been remarked in the several decades because of its disturbance and severity that leading to a serious morbidity and excess mortality in long-term consequences. Although numerous methods have been advocated for treatment an OSA syndrome, no single procedure employed effectively.

Three-dimensional airway models during tidal breathing has been performed in a patient with obstructive sleep apnea and three normal subjects. Segmentation was carried out from CT data initially. Then, the volumetric surface was performed by reverse engineering process and mesh generation was operated after that. Computational modeling for inspiration was operated by employing k - ε turbulence model. For comparison the airflow characteristics, cross-sectional areas, velocity, pressure distribution, and wall shear stress of OSA and healthy models were illustrated. The air flow behaviors are compared in major interested concepts which are velocity magnitude, pressure contour and wall shear stress of all subjects. Moreover, cross-sectional areas are compared as well. Simulation results were illustrated in as follows. Figure 5.1 shows contour plot of velocity streamline of all subjects at mid sagittal plane and figure 5.2 illustrates plot maximum velocity magnitude (m/s) at constricted area of entire models. Figure 5.3 depicts pressure gradients of inspired flow among subjects at mid sagittal plane. Besides, Figure 5.4 indicates comparative significant pressure distribution results from CFD at narrowed area. Then wall shear stress contours in each geometry were compared in figure 5.5. In addition, figure 5.6 also demonstrates comparative wall shear stress contours in all geometries.

Following the mentioned results, velocity magnitudes and streamline indicated uniform flow pattern inside healthy subjects, whereas in OSA patient are different, especially in oropharynx part. In fact, velocity increase dominantly in patient associated with OSA because of narrowing airway from obstruction, 17.37 m/s is found at the most narrowest region. As a result, the internal pressure distribution exhibits larger negative pressure than another. Moreover, wall shear stress in OSA patient is remarkable. Owing to narrowing airway, WSS rises up obviously this could refer to patient's illness such as soreness or bleeding inside upper airway.

Figure 5.7 shows a chart of cross-sectional areas (CSA) comparison from data in Table 5.1. It can be seen that OSA patient has airway more stricture than healthy subjects around oropharynx section. The result claims clearly those upper airway are different, similarly to the different airway boundaries in three-dimensional models and

CFD simulation results. Moreover, figure 5.8 shows the process obtaining 3D airway geometry of patient who having OSA reconstructed from CT images during sleep and having apnea. Similar to CSA, patient associated with OSA is more likely have narrower pharyngeal airway than normal subjects throughout awaking, sleeping and having apnea. It is also obvious found that when the airway obstruct, the OSA patient may get snoring and arousal through the night. This frequently lack of the oxygen blood lead to a minor illness to violent mortality disorders.

This study performed steady k - ε turbulence approach to illustrate characteristics of airflow for comparison between OSA and healthy subject was found to be acceptable as compared to earlier researches. Maximum velocity in our study was 11.11m/s, pressure was -160Pa, and WSS was 2.47Pa for OSA patient, Negative pressure of airflow cause airway predisposition to collapse .Even though k - ε turbulence model cannot demonstrated the dynamics flow like LES of DNS, it may be sufficient for numerous-cases investigation, This could be provided valuable data with performed-time less than LES or DNS. Previous works on CFD simulation can provide abnormally anatomical airway and flow behavior as well as our study. However, integrated CFD-CT technique applied with PSG data are more highly effective technique for diagnostic approach. Physicians can analyze through upper airway of OSA patient all of sleep stages; wake, sleep, and apnea. Therefore, they can find out the cause of constricted site, varies in pathology of each patient. Moreover, 3D airway model can give an idea for virtual surgery (pre- and post- treatment clinical follow-up).

In summary, it is a first step for improving diagnostic technique in OSA patient, especially in Thai. Increasing number of patients associated with OSA and varies in their severity such as mild or moderate OSA, should be investigated for further understanding. Additionally, comparison CFD results while patient was sleeping, having apnea and awaking should be also examined for better comprehension.

CHAPTER VI

Conclusions

6. 1 Summary

Computational fluid dynamics is well cooperated with CT images and PSG data such a tool in advanced diagnostics and could be yield terrific advantages in treatment planning. Integrated CFD-CT technique with PSG is the new research methodology for develop treatment planning more accurate and also reduce cost in diagnosis.

This study can exhibit three-dimensional geometries and analyze cross-sectional area of human upper airways among patient with OSA and three healthy subjects. In addition, CFD results which are velocity magnitudes, pressure drop, and wall shear stress can illustrated fluid dynamic phenomena effectively. It can be seen that OSA patient has aggressive flow more than normal subjects obviously because of narrower airway. Moreover, larger negative pressure and increased wall shear stress are present in that narrower area as well.

Notwithstanding, It is the first step to combined engineering process and human biology in Thai. More OSA patients ought to investigate for outstanding airflow pattern in Thai patients. Besides, for obtaining an accuracy simulation results, we should carefully perform especially in segmentation process. Manually segmentation should be done and carried out following the physician.

Medical imaging modalities, such as MRI, nowadays, provide a quality image and non-invasive diagnosis. Such interesting study should be performed with CFD technique to develop effective assisted tool for physicians in the future.

6. 2 Suggestions for Future Work

6.2.1. Comparison for more OSA patients in Thai good for explore.

6.2.2. Study the airflow in each stages of sleep during wake, sleep, and apnea should be tested for further detailed.

6.2.3. Follow-up monitoring of specific OSA patient should be investigated after surgical treatment.

6.2.4. Validation with experimental model is worth for better understanding the airflow mechanism.

References

[1] American Academy of Sleep Medicine. 2005. **American Academy of Sleep Medicine International classification of sleep disorders: Diagnostic and Coding Manual.** Westchester. IL. 2nd edition.

[2] Isono S, Remmers JE, Tanaka A, Sho Y, Sato J, Nishino T. 1997. "Anatomy of pharynx in patients with obstructive sleep apnea and in normal subjects." **J Appl Physiol.** 82(4):1319–1326.

[3] Kiely JL, McNicholas WT. 2000. "Cardiovascular risk factors in patients with obstructive sleep apnoea syndrome." **Eur Respir J**. 16:128–133.

[4] Parra O, Arboix A, Montserrat JM, et al. 2004. "Sleep-related breathing disorders: impact on mortality of cerebrovascular disease." **Eur Respir J**. 24:267–272.

[5] Yaggi HK, Concato J, Kernan WN, et al. 2005. "Obstructive sleep apnea as a risk factor for stroke and death." **N Engl J Med.** 353:2034–2041.

[6] C. L. Marcus. 2001. "Sleep-disordered breathing in children." **Am J Respir Crit Care Med**. 164:16-30.

[7] AARC-APT (American Association of Respiratory Care-Association of Polysomnography Technologists). 1995. "Clinical practice guideline". Polysomnography. **Respir Care.** 40:1336.

[8] Woodhead CJ, Allen MB. 1994. "Nasal surgery for snoring." **Clin Otolaryngol**. 19:41-44.

[9] Epstein LJ, Kristo D, Strollo PJ Jr, et al. 2009. "Clinical guideline for the evaluation, management and long-term care of obstructive sleep apnea in adults." **J Clin Sleep Med**. 5: 263–276.

[10] Sullivan CE, Issa FG, Berthon-Jones M, et al. 1981. "Reversal of obstructive sleep apnoea by continuous positive airway pressure applied through the nares." **Lancet**. 1: 862–865.

[11] Vanderveken OM, Devolder A, Marklund M, et al. 2008. "Comparison of a custom-made and a thermoplastic oral appliance for the treatment of mild sleep apnea." **Am J Respir Crit Care Med**. 178:197–202.

[12] Beekhuis, G. J. 1976. "Nasal obstruction after rhinoplasty: etiology, and techniques for correction." **The Laryngoscope.** 86(4):540–548.

[13] Friedman, M., Wilson, M., Lin, H.-C., Chang, H.-W. 2009. "Updated systematic review of tonsillectomy and adenoidectomy for treatment of pediatric obstructive sleep apnea/hypopnea syndrome." **Otolaryngology-Head and Neck Surgery**. 140(6):800–808.

[14] H.K. Versteeg and W. Malalasekera. 2007. **An Introduction to Computational Fluid Dynamics: The Finite Volume Method**. 2nd Edition, Prentice Hall.

[15] D.J Doorly, D.J Taylor, A.M Gambaruto, R.C Schroter and N Tolley. 2008. "Nasal architecture: form and flow." **Phil. Trans. R. Soc. A**. 366:3225-3246.

[16] Chen XB, Lee HP, Chong VF, Wang de Y. 2010. "A computational fluid dynamics model for drug delivery in a nasal cavity with inferior turbinate hypertrophy." **J Aerosol Med Pulm Drug Deliv.** 23(5):329-38.

[17] Chun Xu, SangHun Sin, Joseph M. McDonough, Jayaram K. Udupa, Allon Guez, Raanan Arens, David M. Wootton. 2006 "Computational fluid dynamics modeling of the upper airway of children with obstructive sleep apnea syndrome in steady flow." **Journal of Biomechanics**. 39: 2043-2054.

[18] C. C. Yu, H. D. Hsiao, L. C. Lee, C. M. Yao, N. H. Chen, C. J. Wang, Y. R. Chen. 2009. "Computational fluid dynamics study on obstructive sleep apnea syndrome treated with maxillomandibular advancement**." Journal of Craniofacial Surgery**.20(2):426–430.

[19] Goutham Mylavarapu et al. 2009. "Validation pf computational fluid dynamics methodology used for human upper airway flow simulations." **Journal of Biomechanics**. 42:1553-1559.

[20] Y. Fan, L. K. Cheung, M. M. Chong, H. D. Chua, K. W. Chow, and C. H. Liu. 2011. "Computational Fluid Dynamics Analysis on the Upper Airways of Obstructive Sleep Apnea Using Patient – Specific Models." **IAENG International Journal of Computer Science.** 38:4.

[21] Mihai Mihaescu, Goutham Mylavarapu, Ephraim J. Gutmark, Nelson B. Powell. 2011. "Large Eddy Simulation of the pharyngeal airflow associated with Obstructive Sleep Apnea Syndrome at pre and post-surgical treatment." **Journal of Biomechanics**. 44:2221-2228.

[22] Muntarbhorn K. 1998. "Uvulopalatopharyngoplasty for exces-sive snoring, daytime sleepiness, sleep apnea and hypertension." **Intern. Med. (Thailand)**. 4(3):108–11.

[23] Muntarbhorn K, Kunachak S. 1999. "Palatal surgery, uvulopalatopharyngoplasty and laser-assisted uvulopalatoplasty for snorers: a chronological perspective." **J Int Coll Surg Thai.** 40:11-6.

[24] Charoenpan P, Thanakitcharu S, Muntrabhorn K, Kunachak S, Boongird P, Likittanasombat K, Suwansathit W. 1999. "Sleep apnoea syndrome in Ramathibodi Hospital: Clinical and polysomnographic baseline data." **Respirology**. 4:371–374.

[25] Pongcharusathit C, Kunachak S, Kulapadittharom B, Bhongmakaphat T, Chewaruangroj W, Praneetvatakul V, et al. 2003. "Clinical predictors of

obstructive sleep apnea syndrome in Thai males." **Thai J Otolaryngol Head Neck Surg.** 4:14-21.

[26] NHLBI: Health Information for the Public. U.S. Department of Health and Human Services. May 2009. **"Sleep Apnea: What Is Sleep Apnea?"**.

[27] Morgenthaler TI, Kagramanov V, Hanak V, Decker PA. Sep. 2006. "Complex sleep apnea syndrome: is it a unique clinical syndrome?" **Sleep** 29 (9): 1203–9. PMID 17040008. Lay summary – Science Daily.

[28] W. De Backer. 2006. "Obstructive sleep apnea–hypopnea syndrome— definitions and pathophysiology." W.J. Randerath, B.M. Sanner, V.K. Somers (Eds.), **Sleep Apnea-Current Diagnosis and Treatment**, S. Karger AG, Basel, Switzerland: 90–96.

[29] N.collop. 2007. "The effect of obstructive sleep apnea on chronic medical disorders." **Cleveland clinic journal of medicine**. 74(1):72-78, Florida, SA.

[30] Young T, Skatrud J, Peppard P. 2004. "Risk factors for obstructive sleep apnea in adults." **The Journal of the American Medical Association.** 291:2013–2016.

[31] Kapsimalis F, Kryger MH. 2002. "Gender and obstructive sleep apnea syndrome, part 1: clinical features." **Sleep.** 25(4):412-419.

[32] Young T, Palta M, Dempsey J, et al. 1993. "The occurrence of sleep-disordered breathing among middle-aged adults." **N Engl J Med**. 328:1230-5.

[33] Young T, Evans L, Finn L, Palta M. 1997. "Estimation of the clinically diagnosed proportion of sleep apnea syndrome in middle-aged men and women." **Sleep.** 20:705-6.

[34] Redline S, Tishler PV, Hans MG, Tosteson TD, Strohl KP, Spry K. 1997. "Racial differences in sleep-disordered breathing in African-Americans and Caucasians." **American Journal of Respiratory and Critical Care Medicine.** 155(1):186-92.

[35] Redline S, et al. 1999. "Risk Factors for Sleep-Disordered Breathing in Children." **American Journal of Respiratory and Critical Care Medicine**. 159:1527-32.

[36] I. Edward Alcamo; John Bergdahl. 2003. **Anatomy Coloring Workbook. The Princeton Review:** 238.

[37] url: [http://resource.deyogroup.com/347/Throat.png]

[38] Mayo Clinic. June 2010. "Sleep Apnea: Risk Factors."

[39] ANSYS Inc. Nov. 2011. **ANSYS FLUENT Theory Guide.** Release ver 14.0.

[40] Launder, B. E. and Spalding, D. B. 1974. "The Numerical Computation of Turbulent Flows." **Comput. Methods Appl. Mech. Eng**. 3:269–289.

[41] Robert Eymard, Thierry Galloet and Raphaele Herbin. 2003. **Finite Volume Methods. Handbook of Numerical Analysis** P.G. Ciarlet, J.L. Lions eds, (7):713-1020

[42] John D. Anderson. 1995. **Computational Fluid Dynamics**. 1st Edition, McGraw-Hill,

Biography

Personal Information

Name	Chompunuch Sarasaen
Nationality	Thai
Date of birth	July 15, 1988
Place of birth	Bangkok, Thailand
E-mail address	chompunuch.sarasaen@yahoo.com

Education

Bachelor's degree

Field	Bachelor of Science (2007-2010)
University	Mahidol University
Faculty	Medical Technology
Major	Radiological Technology

Research Interests

Computational fluid dynamic, numerical simulation, airflow simulation, medical imaging, obstructive sleep apnea syndrome.

List of Publications

1. Chompunuch Sarasaen, Khaisang Hemtiwakorn, Jiraporn Laothamatas, Manas Sangworasil, Chuchart Pintavirooj, **"Computational Fluid Dynamics of Human Upper Airway Applied with Obstructive Sleep Apnea - A Preliminary Study"**, *The 4th Biomedical Engineering Conference (BMECON 2012)*, pp:82-86
2. Chompunuch Sarasaen, Khaisang Hemtiwakorn, Thongchai Bhongmakapat, Jiraporn Laothamatas, Chuchart Pintavirooj, **"Computational Fluid Dynamic (CFD) in Thai Patient with Obstructive Sleep Apnea Syndrome (OSAS) - A Case Report: Comparative Study Between Healthy and OSA Subject"**, *The 5th Biomedical Engineering International Conference (BMEiCON-2012)*, Vol.5, pp: 95-96